Biogeosciences, 10, 7109–7131, 2013
www.biogeosciences.net/10/7109/2013/
doi:10.5194/bg-10-7109-2013

Biogeosciences Open Access

The effect of vertically resolved soil biogeochemistry and alternate soil C and N models on C dynamics of CLM4

C. D. Koven[1], W. J. Riley[1], Z. M. Subin[1,2], J. Y. Tang[1], M. S. Torn[1], W. D. Collins[1], G. B. Bonan[3], D. M. Lawrence[3], and S. C. Swenson[3]

[1]Lawrence Berkeley National Lab (LBNL), Berkeley, CA, USA
[2]Now at Princeton Environmental Institute, Princeton, NJ, USA
[3]National Center for Atmospheric Research (NCAR), Boulder, CO, USA

Correspondence to: C. D. Koven (cdkoven@lbl.gov)

Received: 9 April 2013 – Published in Biogeosciences Discuss.: 23 April 2013
Revised: 22 August 2013 – Accepted: 23 August 2013 – Published: 10 November 2013

Abstract. Soils are a crucial component of the Earth system; they comprise a large portion of terrestrial carbon stocks, mediate the supply and demand of nutrients, and influence the overall response of terrestrial ecosystems to perturbations. In this paper, we develop a new soil biogeochemistry model for the Community Land Model, version 4 (CLM4). The new model includes a vertical dimension to carbon (C) and nitrogen (N) pools and transformations, a more realistic treatment of mineral N pools, flexible treatment of the dynamics of decomposing carbon, and a radiocarbon (^{14}C) tracer. We describe the model structure, compare it with site-level and global observations, and discuss the overall effect of the revised soil model on Community Land Model (CLM) carbon dynamics. Site-level comparisons to radiocarbon and bulk soil C observations support the idea that soil C turnover is reduced at depth beyond what is expected from environmental controls for temperature, moisture, and oxygen that are considered in the model. In better agreement with observations, the revised soil model predicts substantially more and older soil C, particularly at high latitudes, where it resolves a permafrost soil C pool. In addition, the 20th century-C dynamics of the model are more realistic than those of the baseline model, with more terrestrial C uptake over the 20th century due to reduced N downregulation and longer turnover times for decomposing C.

1 Introduction

Soil organic matter (SOM), which cycles with the atmosphere on a decadal to centennial timescale, is the largest reservoir of carbon in the terrestrial earth systems. Because of the dependence of soil heterotrophic respiration and the resulting CO_2 release on environmental conditions, climate change may lead to potentially large positive feedbacks with the atmosphere (Jenkinson et al., 1991). The current generation of coupled carbon-climate models have high uncertainty in the magnitude of carbon cycle feedbacks (Friedlingstein et al., 2006; Arora et al., 2013), and a dominant source of this uncertainty is associated with SOM sensitivity to environmental change (Jones et al., 2003). In addition to a direct role in the global C cycle through SOM decomposition and CO_2 production, SOM plays a crucial role in soil nutrient feedbacks – in particular, C-N couplings – because decomposing SOM provides mineralized N for vegetation growth. These feedbacks have been shown to play a crucial but poorly constrained role in Earth System Models (ESMs) that include a representation of these processes (Thornton et al., 2009; Wang et al., 2010; Zaehle et al., 2010).

The actual uncertainty in the role of SOM in terrestrial carbon feedbacks may be greater than that estimated from multi-model ESM ensembles, given the high degree of conceptual similarity between the SOM dynamics as represented in these models. Despite discretizing soils vertically for soil physics (moisture and energy) calculations, ESMs have typically represented SOM biogeochemistry with a single-layer

box-modeling approach. Typically, a fixed SOM profile is used for modeling the effect of soil climate on SOM turnover, but the lower boundary of the SOM pool is left poorly defined. This approach assumes that deeper SOM does not play an active role in carbon cycling, and that vertical variations in the upper soil can be adequately represented as a single equivalent box. However, large quantities of SOM below the surface layers have been observed in a variety of soils, and may cycle on decadal timescales (Baisden and Parfitt, 2007; Koarashi et al., 2012). In particular, permafrost soils contain enormous quantities of SOM C below 1m depth (Ping et al., 2008; Tarnocai et al., 2009), and since a main limitation to the decomposition of this material is the cold, anoxic condition at depth, warming could potentially make permafrost SOM vulnerable to decomposition. ESMs that take the permafrost C pool into account predict net CO_2 losses under warming (Koven et al., 2011; Schaefer et al., 2011), as opposed to net CO_2 gains under warming predicted in ESMs that do not explicitly represent permafrost C (Qian et al., 2010).

The purpose of this paper is to describe a new soil biogeochemistry model (Fig. 1), which represents the vertically resolved C and N cycles responsible for SOM and litter turnover and plant-soil nutrient interactions. This model is integrated in the Community Land Model, version 4 (CLM4) (Oleson et al., 2010; Lawrence et al., 2011), which is a component of the Community Earth System model, version 1 (CESM1). Here, we describe the formulation of this model and the sensitivity of model behavior to parameters. We also make a comparison between model predictions and observations, and a comparison between different model versions of the transient behavior of the CLM C cycle during the period 1955–2004.

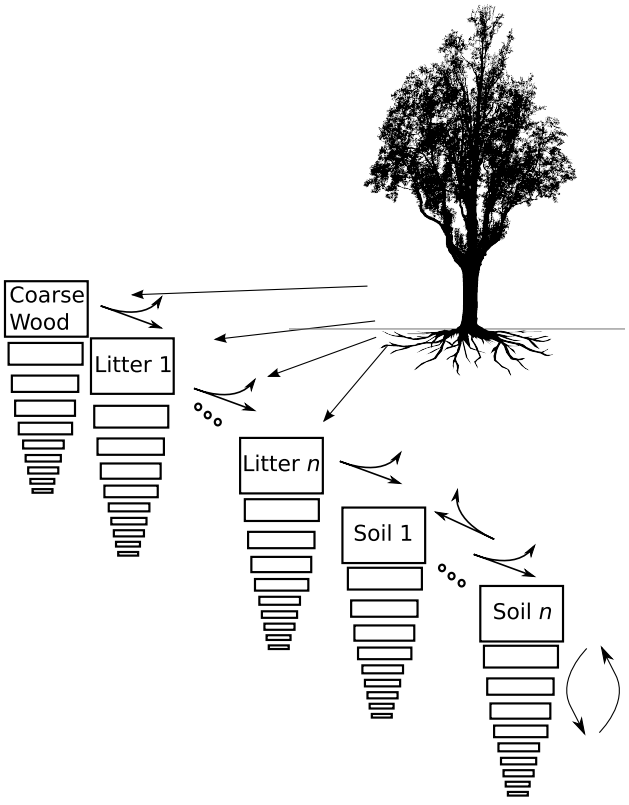

Fig. 1. Schematic of vertically resolved soil C and N model in CLM4.5. A flexible framework for defining decomposing C and N pools has been added to the model. Plant inputs of C and N to coarse woody debris (CWD) and litter pools. Decomposition of CWD and litter leads to heterotrophic respiration and formation of SOM. Each decomposing C and N pool is defined at each soil vertical level, with vertical mixing within each pool.

2 Model description

2.1 C and N decomposition cascade structure

SOM decomposition is a complex process in which plant inputs are consumed, respired and recycled by a complex web of soil decomposers, and stabilized and transported by a variety of physical processes. Many soil models have been developed to track organic material from plant inputs to soil organic matter, including models of continuous change and discrete lability bins (Bosatta and Agren, 1991). Here we use the discrete bin concept, with modified first-order decay of decomposing organic material pools. In this model representation, organic material is initially passed from plant pools to litter and coarse woody debris (CWD) pools. Subsequently it is decomposed and passed through a cascade of different pools, and is partially respired at each step. Thus, the change in carbon pools for the base, single-layer model is as follows:

$$\frac{\partial C_i}{\partial t} = R_i + \sum_{j \neq i} (1 - r_j) T_{ji} k_j C_j - k_i C_i, \quad (1)$$

where C_i is the carbon content of pool i ($\mathrm{kg\,C\,m^{-2}}$), R_i are the plant inputs into pool i ($\mathrm{kg\,C\,m^{-2}\,s^{-1}}$), k_i is the decay constant for pool i ($\mathrm{s^{-1}}$); and T_{ji} is the fraction of carbon from pool j that is directed toward pool i with a fraction r_j lost as respiration. The standard CLM4.0-CN decomposition cascade is described by Thornton and Rosenbloom (2005); in the revised model we generalize the structure of the model so that different structural and parametric representations of the soil and litter decomposition cascade can be considered. Here, we compare two possible decomposition cascades (Fig. 2 and Tables 1 and 2): the standard CLM-CN model, and an alternate decomposition cascade from the Century soil model (Parton et al., 1988).

Because CLM4 is a coupled C and N model, organic N pools follow an analogous path to the C pools, with mineralization or immobilization of soil mineral N occurring

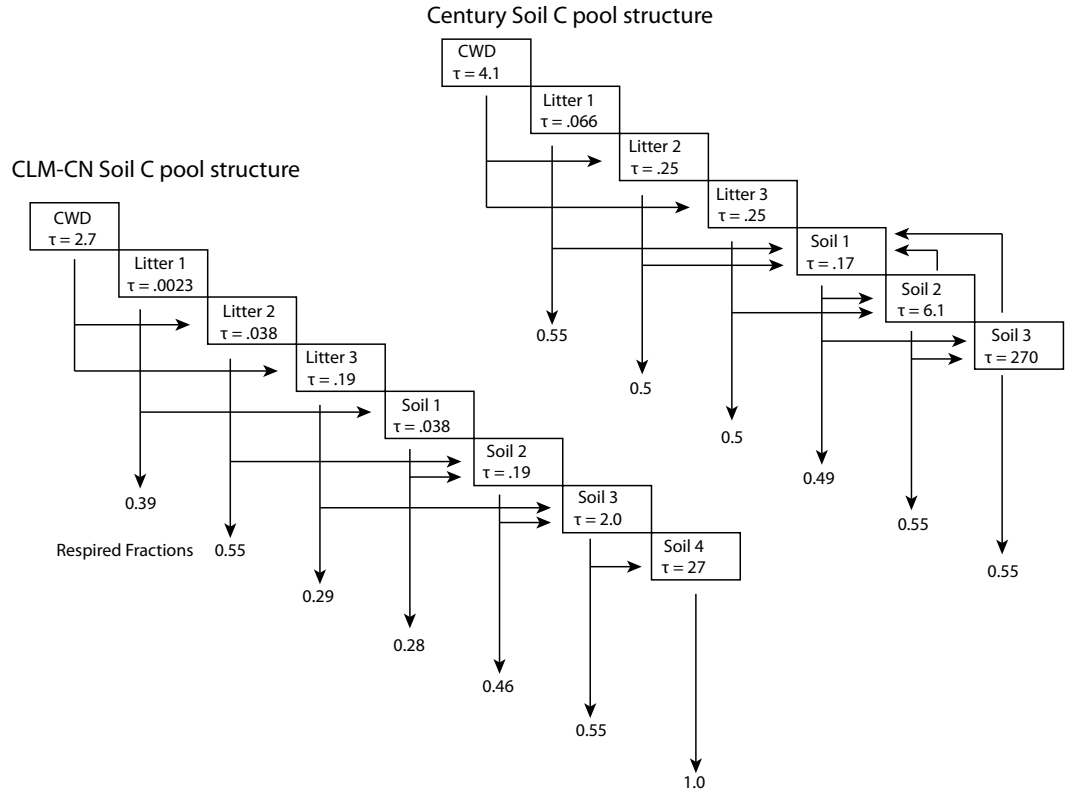

Fig. 2. Comparison of 2 decomposing pool cascade structures and parameters used in this study. Turnover times (in boxes) are in years. Numbers at end of arrows are respired fractions. Summarized information in Tables 1 and 2.

along each step of the decomposition cascade (Thornton and Rosenbloom, 2005),

$$\mathrm{NF}_{ji} = \frac{k_j C_j \left(1 - r_j - \frac{\mathrm{CN}_i}{\mathrm{CN}_j}\right)}{\mathrm{CN}_i}, \tag{2}$$

where NF_{ji} is the net nitrogen flux (positive NF_{ji} indicates immobilization, negative NF_{ji} indicates mineralization), and CN_j and CN_i are the upstream and downstream pool C : N ratios for a given transition $j \to i$. The model is structured such that each pool that is downstream of a decomposition step with r_j greater than 0 is assigned a fixed C : N ratio, while the litter pools that only receive C and N from plants or coarse woody debris (CWD), which decays to litter with no respiratory flux, have floating C : N ratios based on the C : N ratios of the plant inputs. When more nitrogen is released by SOM mineralization than is required for immobilization by litter decomposition or plant uptake, this N is added to the soil mineral N pools; when demand exceeds supply, both the plant N uptake (and, consequently, the photosynthetic C uptake, which is stoichiometrically bound to N availability) and the litter decomposition with its associated N immobilization are reduced (Thornton and Rosenbloom, 2005).

2.2 Vertical soil biogeochemistry model

2.2.1 Vertical discretization and mixing

In the new model, we modify Eq. (1) to have a vertical dimension z and transport across that dimension:

$$\frac{\partial C_i(z)}{\partial t} = R_i(z) + \sum_{j \neq i} (1 - r_j) T_{ji} k_j(z) C_j(z) - k_i(z) C_i(z) + \frac{\partial}{\partial z}\left(D(z)\frac{\partial C_i}{\partial z}\right) + \frac{\partial}{\partial z}\left(A(z) C_i\right) \tag{3}$$

, where carbon content C_i is now defined volumetrically ($\mathrm{kg\,C\,m^{-3}}$), plant inputs R_i ($\mathrm{kg\,C\,m^{-3}\,s^{-1}}$) are distributed over the profile, decomposition constant k_i is defined at each model level, and we add an advective-diffusive soil C transport component, with diffusivity D ($\mathrm{m^2\,s^{-1}}$) and advection A ($\mathrm{m\,s^{-1}}$). The vertical dimension requires three new sets of parameters: the initial distribution of C and N inputs, the advection and diffusion terms, and a possible additional depth dependence to turnover time. We discuss the implications of adding the vertical dimension for SOC decomposition and uncertainty in the additional parameters below.

CLM4 already includes vertical discretization of soil temperature and moisture, with a default vertical grid of 15 levels, the bottom 5 of which are used for temperature

Table 1. Pool characteristics for the two decomposition structures used in this paper. Turnover times, τ, are for reference conditions of 25C and no moisture or oxygen limitations. CN_i is the C : N ratio for each pool. A_i is the factor of accelerated decomposition used for each pool during the model equilibration procedure.

Pool Name	τ (yr)	CN_i	A_i
CN			
CWD	2.7	–	1
Litter 1	0.0023	–	1
Litter 2	0.038	–	1
Litter 3	0.19	–	1
Soil 1	0.038	12	1
Soil 2	0.19	12	1
Soil 3	2.0	10	5
Soil 4	27	10	70
Century-based			
CWD	4.1	–	1
Litter 1	0.066	–	1
Litter 2	0.25	–	1
Litter 3	0.25	–	1
Soil 1	0.17	8	1
Soil 2	6.1	11	15
Soil 3	270	11	675

Table 2. Decomposition cascades for the two structures used in this paper.

Transition Pools	T_{ji}	r_j
CN		
CWD → L2	0.76	0
CWD → L3	0.24	0
L1 → S1	1	0.39
L2 → S2	1	0.55
L3 → S3	1	0.29
S1 → S2	1	0.28
S2 → S3	1	0.46
S3 → S4	1	0.55
S4 → atm	1	1.0
Century-based		
CWD → L2	0.76	0
CWD → L3	0.24	0
L1 → S1	1	0.55
L2 → S1	1	0.5
L3 → S2	1	0.5
S1 → S2	f(txt)	f(txt)
S1 → S3	f(txt)	f(txt)
S2 → S1	0.93	0.55
S2 → S3	0.07	0.55
S3 → S1	1	0.55

calculations only (Lawrence et al., 2008). The grid level thickness increases exponentially, so that the soil temperature grid has a maximum depth of 42 m, while the soil hydrological grid has a maximum depth of 3.8 m. The change here adopts the same grid structure, but updates the soil C and N cycles at each of the levels on which soil moisture balance is calculated. A major uncertainty is created by the fact that we do not have information on actual soil depths globally, and so we assume that soil carbon and nitrogen cycling can take place to the 3.8 m depth everywhere.

A similar vertical distribution of soil biogeochemical cycling was introduced into the RothC carbon model (Jenkinson and Coleman, 2008; Jenkinson et al., 2008). We follow a conceptually similar approach here, although an important difference between RothC and the one described here is that the RothC model assumes layers of defined thickness and discrete processes based on those layer thicknesses; here we define a model that is independent of vertical resolution and thus can be compared more easily with observation-based estimates of, e.g., soil mixing rates. Another recent approach to creating a prognostic vertically resolved SOM model was proposed by Braakhekke et al. (2011); our approach here is similar, although there are differences: we do not differentiate between different physical layers by defining horizon types, and we assume that all SOM and litter pools have the same transport properties. Future work will include separately modeling the differences in biogeochemical and physical effects of prognostically defined organic and mineral horizons, and more explicitly tying tracer vertical transport to the movement of water through soils. This latter effect is investigated thoroughly in CLM using CLM4-BeTR (Biogeochemical Transport and Reactions) (Tang et al., 2013); here we assume only slow transport of adsorbed phases.

2.2.2 Decomposition rates

In the classical 0-D SOM modeling approach, the moisture and temperature environmental controls are diagnosed over some surface interval, typically 30 cm as was done for CLM4.0. This approach does not allow for differing environmental controls across the vertical profiles, as is the case in soils where deep decomposition is inhibited by freezing and/or anoxia. In the new model, decomposition rates are defined at each model level as the product of an intrinsic turnover time for each pool, with environmentally controlled rate modifiers:

$$k_i = k_{0,i} r_T r_w r_O r_z, \quad (4)$$

where $k_{0,i}$ is the intrinsic turnover time for each pool (yr^{-1}; Table 1), r_T is the temperature rate modifier, r_w is the moisture modifier, r_O is the oxygen modifier, and r_z is the depth modifier (all the modifiers are dimensionless scale factors). We assume that each of these rate modifiers act equally on all soil pools, and that no interactions between these rate modifiers exist. There is considerable uncertainty on these points,

for example with the carbon quality temperature hypothesis (Davidson and Janssens, 2006), or different temperature dependence for oxic and anoxic soils; we do not investigate these uncertainties here.

CLM4 prognoses soil moisture and temperature at each model level, and thus the environment-specific rate modifier terms are all calculated at each model level. The temperature effect on decomposition, r_T, follows a standard exponential relationship with a Q_{10} of 1.5, in agreement with ecosystem-level observed rates (e.g. Mahecha et al., 2010). The moisture sensitivity is a function of soil matric potential ψ (Andrén and Paustian, 1987),

$$r_w = \frac{\log\left(\frac{\psi_{\min}}{\psi}\right)}{\log\left(\frac{\psi_{\min}}{\psi_{\max}}\right)}, \quad (5)$$

where r_w is the rate scalar for moisture limitation, equal to 0 below $\psi_{\min}$ and 1 above $\psi_{\max}$, with $\psi_{\min} = -10$ MPa and $\psi_{\max}$ equal to the saturated soil matric potential. The Q_{10} formulation, as well as other temperature functions such as the Arrhenius equation, varies smoothly across the range of frozen and unfrozen temperatures, and thus a single Q_{10} or Arrhenius value cannot capture the observed sharp reduction in decomposition that occurs across the freezing point. One way of including the freeze inhibition is to use either a threshold function or a second, much larger "frozen Q_{10}" value below the freezing point, though there is considerable uncertainty about the functional form and magnitude of this effect (Koven et al., 2011). Because the freeze inhibition of decomposition is essentially a liquid water limitation, CLM calculates this effect directly via cryosuction, which is the explicit temperature dependence of soil water matric potential below the freezing point, using the supercooled water formulation of Niu and Yang (2006):

$$\psi(T) = -\frac{L_{\mathrm{f}}(T - T_{\mathrm{f}})}{10^3 T} \quad (6)$$

where L_{f} (J kg^{-1}) is the latent heat of fusion, and T_{f} (K) is the freezing temperature of water. Thus the total temperature limitation below the freezing point is equal to the product of the Q_{10}-based direct limitation and the temperature-dependent moisture limitation. For $\psi_{\min}$ of -10 MPa in Eq. (5), this formulation predicts zero respiration rates below -8 °C.

In addition to respiration rate limitation by temperature and moisture, we include a limitation by oxygen availability, r_O. Soil O_2 concentrations are calculated using the Riley et al. (2011) scheme for vertical diffusion and consumption by respiration and methanotrophy. Where oxygen availability is insufficient to meet oxygen demands, respiration rates are scaled down to consume only the available O_2, with a minimum oxygen limitation of 0.2 based on decomposition rates in anaerobic soils. This value lies between estimates of 0.025–0.1 (Frolking et al., 2001), and 0.35 (Wania et al., 2009); the large range of these estimates poses an uncertainty for wetland carbon storage. Riley et al. (2011) calculate trace gas profiles for both upland and wetland soils; in this study, we use only the calculated upland O_2 concentrations in the base case. Anoxia can still develop in this framework – for example, where infiltration is limited by permafrost layers, or where rainfall rates are high.

Lastly, a possible explicit depth dependence, r_z, can be applied to soil C turnover times to account for processes other than temperature, moisture, and anoxia that can limit decomposition. This depth dependence of decomposition was shown by Jenkinson and Coleman (2008) to be an important term in fitting total C and ^{14}C profiles, and implies that unresolved processes, such as priming effects, microscale anoxia, soil mineral surface and/or aggregate stabilization may be important in controlling the fate of carbon at depth. Here, we include these unresolved depth controls via an exponential decrease in the soil turnover time with depth:

$$r_z = \exp\left(-\frac{z}{z_\tau}\right) \quad (7)$$

where z_τ is the e-folding depth of intrinsic turnover rates. We explore the predicted C and ^{14}C profiles' sensitivity to z_τ in comparison with site data.

2.2.3 Vertical mixing

Observations of the ^{14}C age and lability of soil organic matter suggest that near-surface incorporation of fresh carbon, with slow diffusive or advective transport deeper into the soil, leads to the presence of deep soil organic matter (O'Brien and Stout, 1978; Elzein and Balesdent, 1995; Baisden et al., 2002). In the vertically resolved soil biogeochemistry in CLM4, we assume that vertical mixing can be modeled using an advective-diffusive transport, with advective transport occurring as a result of transport by infiltrating soil water or deposition of surface material, and diffusive transport occurring as a result of mixing by biological or physical processes. These effects are represented by the last two terms in Eq. (3).

Rates of vertical mixing for various processes have been estimated by a number of researchers (Table 3). In temperate soils, these rates span a range of 0.3–17 cm^2 yr^{-1} for diffusive mixing and 0.1–0.5 mm yr^{-1} for advection, when both advection and diffusion are considered; when only advection is considered, the advective mixing rate spans the range of 1–5 cm yr^{-1}. We found no studies that reported diffusive or advective mixing rates for cryoturbation in permafrost soils. We assume here (1) a base diffusive bioturbation mixing rate of 1 cm^2 yr^{-1} for non-permafrost, (2) a cryoturbation mixing rate of 5 cm^2 yr^{-1} for permafrost soils, which is in the middle of the range used by Koven et al. (2011), and (3) a baseline advective mixing rate of 0 mm yr^{-1}; to estimate the impact of uncertainty in these parameters, we conduct sensitivity tests by perturbing these parameters away from these base estimates and examining the model response.

Table 3. The literature-reported values of SOM vertical mixing rates.

Reference	diffusion rate	advection rate	location	depth	ecosystem	process	how inferred
Elzein and Balesdent (1995)	5.15 $cm^2\ yr^{-1}$	0.13 $mm\ yr^{-1}$	Kattinkar, India		forest	bioturbation	^{14}C
Elzein and Balesdent (1995)	16.58 $cm^2\ yr^{-1}$	0.34 $mm\ yr^{-1}$	Para, Brazil		forest	bioturbation	^{14}C
Elzein and Balesdent (1995)	5.29 $cm^2\ yr^{-1}$	0.48 $mm\ yr^{-1}$	Bahia, Brazil		forest	bioturbation	^{14}C
Elzein and Balesdent (1995)	0.94 $cm^2\ yr^{-1}$	0.6 $mm\ yr^{-1}$	Bezange, France		forest	bioturbation	^{14}C
Elzein and Balesdent (1995)	1.48 $cm^2\ yr^{-1}$	0.42 $mm\ yr^{-1}$	Marly, France		forest	bioturbation	^{14}C
Bruun et al. (2007)	0.71 $cm^2\ yr^{-1}$	0.081 $mm\ yr^{-1}$	Sweden				^{14}C
O'Brien and Stout (1978)	13 $cm^2\ yr^{-1}$		New Zealand	0–1 m	pasture		^{14}C
Jarvis et al. (2010)	0.3 $cm^2\ yr^{-1}$		Sweden	0–50 cm	forest	bioturbation	^{137}Cs
Baisden et al. (2002)		0.01–0.4 $cm\ yr^{-1}$	California		grassland	bioturbation	^{14}C
Baisden and Parfitt (2007)		0.6, 0.09, 0.019	California		grassland	bioturbation	^{14}C
Baisden and Parfitt (2007)		0.06, 0.13, 0.025	California		grassland	bioturbation	^{14}C
Baisden and Parfitt (2007)		0.05 $cm\ yr^{-1}$	New Zealand		grassland	bioturbation	^{14}C
Yoo et al. (2011)		1–5 $cm\ yr^{-1}$	Delaware	surface	agro	tillage	^{210}Pb
Yoo et al. (2011)		0.6–1 $cm\ yr^{-1}$	Delaware	20 cm	agro	tillage	^{210}Pb
Yoo et al. (2011)		0.5–0.7 $cm\ yr^{-1}$	Delaware	surface	forest	bioturbation	^{210}Pb
Yoo et al. (2011)		2.2-3.2 $cm\ yr^{-1}$	Delaware	10 cm	forest	bioturbation	^{210}Pb
Heimsath et al. (2002)		0.007–0.026 $cm\ yr^{-1}$	Australia	10–85 cm	forest	hillslope creep	OSL
Kaste et al. (2007)	1–2 $cm^2\ yr^{-1}$		Australia and California		grassland	bioturbation	^{7}Be, ^{210}Pb
Richards and Humphreys (2010)		0.025–0.04 $cm\ yr^{-1}$	Australia	0–5 cm	forest	bioturbation	tile burial

For bioturbation, we assume that diffusivity is constant throughout the soil column. For permafrost soils, we follow the parameterization of cryoturbation mixing by Koven et al. (2009), in which diffusivity is constant through the active layer and decreases linearly to zero at a set depth (here we use 3m) in the permafrost layer. In addition to physical mixing processes, soil materials can be advected through dissolved transport. We do not consider an explicit dissolved organic pool in either of the decomposition cascade structures tested here, thus we do not model the dissolved transport except as a sensitivity test; we note that Tang et al. (2013) examine the effects of dissolved- and gaseous-phase transport on the soil C and N dynamics using the CLM4-BeTR version of CLM4.

2.2.4 Vertical discretization of carbon inputs

We examine several functional forms for distributing C and N inputs from plant roots up through the soil column. CLM4 calculates root distributions for plant water uptake based on a double-exponential function (Zeng, 2001); in principle, however, the vertical profiles of root C and N inputs to soil need not be identical to those of plant water uptake from soil due to differing root lifetimes (Joslin et al., 2006; Riley et al., 2009) for different types of roots. Thus, one hypothesis is that C inputs are proportional to the root profiles used in the water uptake calculations. Another frequently used root depth parameterization is that of Jackson et al. (1996), which uses a single exponential depth function for a variety of plant functional types. To address this uncertainty, we examine the sensitivity of model results to the two root profile parameterizations used above as well as a range of exponential e-folding depths. We distribute surface inputs (leaf, stem, and seed C and N) across a shallow exponential profile (e-folding depth = 10 cm). Below, we discuss below the sensitivity of the predicted natural abundance ^{14}C, the vertical profile of changes in ^{14}C due to bomb enrichment, and the bulk C profiles to the formulation of root C and N input profiles.

2.3 ^{14}C tracer for assessment of age distribution of C pools

In addition to bulk C contents, we include in the modified CLM4 the ability to simulate ^{14}C ratios for all C pools, including the vertical distributions of ^{14}C in soils. For every C transfer, we define an equivalent ^{14}C transfer, with the ^{14}C flux equal to the bulk C flux multiplied by the $^{14}C/C$ ratio of the upstream C pool. In order to compare modeled with observed ^{14}C content, we use the $\delta^{14}C$ and $\Delta^{14}C$ notation (Stuiver and Polach, 1977):

$$\delta^{14}C = \left(\frac{A_s}{A_{abs}} - 1\right) 1000, \tag{8}$$

$$\Delta^{14}C = 1000\left(\left(1 + \frac{\delta^{14}C}{1000}\right)\frac{0.975^2}{\left(1 + \frac{\delta^{13}C}{1000}\right)^2} - 1\right), \tag{9}$$

where $\delta^{14}C$ is the measured isotopic fraction and $\Delta^{14}C$ corrects for mass-dependent isotopic fractionation processes (assumed to be 0.975 for fractionation of ^{13}C by photosynthesis). A_s is the $^{14}C/C$ ratio in a given sample s. We assume a background preindustrial atmospheric $^{14}C/C$ ratio of 10^{-12}, which we use for A_{abs}. For the reference standard A_{abs}, which is a plant tissue and has a $\delta^{13}C$ value of -25 ‰ due to photosynthetic discrimination, $\delta^{14}C = \Delta^{14}C$. For CLM, we would like to use the ^{14}C model independently

of the ^{13}C model, since both require a complete set of all carbon pools and fluxes and are thus computationally demanding to track. The simplest way of doing this is to assume no fractionation in the model, in which case the 0.975 term in Eq. (9) becomes 1 while the δ^{13}C term becomes 0, so that the modeled δ^{14}C equals the modeled Δ^{14}C, which can then be directly compared to observations of fractionation-corrected Δ^{14}C.

For a comparison with historical ^{14}C measurements, we vary the concentration of atmospheric ^{14}C over the 20th century to account for dilution by fossil fuels and the large release by thermonuclear testing. We impose the atmospheric Δ^{14}C concentration shown in Fig. 3, which we calculate by fitting a spline (solid curve) through several observational datasets (dots) that span the 20th century (Levin and Kromer, 2004; Manning and Melhuish, 1994; Nydal and Lövseth, 1996; Turnbull et al., 2007).

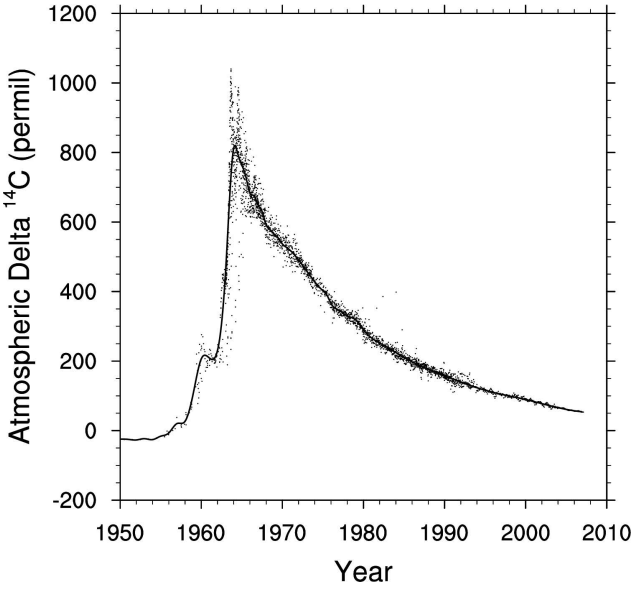

Fig. 3. Atmospheric observations of Δ^{14}C of CO_2 for the period 1950–2010 shown as dots (Levin and Kromer, 2004; Manning and Melhuish, 1994; Nydal and Lövseth, 1996; Turnbull et al., 2007). Spline approximation (solid line) used to force modeled Δ^{14}C of photosynthetic C inputs to CLM during transient 20th century simulations.

2.4 Revised soil N model

2.4.1 Nitrification and denitrification submodels

In the base N cycle in CLM-CN, microbial losses from the soil mineral N pool are parameterized by two sources: a constant fraction (1 %) of N mineralized by decomposing SOM, and a first-order decay ($\tau = 2$ day) of any mineral N not consumed by either plant uptake or N immobilization. We replace the CLM-CN formulation here with a more detailed representation of nitrification and denitrification based on the Century N model (Parton et al., 1996, 2001; Grosso et al., 2000). In this approach, nitrification of NH_4^+ to NO_3^- is a function of temperature, moisture, and pH:

$$F_{\mathrm{nitr,p}} = [\mathrm{NH_4}] k_{\mathrm{nitr}} f(T) f(\mathrm{H_2O}) f(\mathrm{pH}), \quad (10)$$

where $F_{\mathrm{nitr,p}}$ is the potential nitrification rate (prior to competition for NH_4^+ by plant uptake and N immobilization), k_{nitr} is the maximum nitrification rate (10 % day^{-1}, (Parton et al., 2001)), and $f(T)$ and $f(\mathrm{H_2O})$ are rate modifiers for temperature and moisture content. Here we use the same rate modifiers (i.e., r_T, r_w) as are used in the CLM4 decomposition routine. $f(\mathrm{pH})$ is a rate modifier for pH; however, because CLM does not calculate pH, we apply a fixed pH value of 6.5 in the pH function of Parton et al. (1996).

The potential denitrification rate is co-limited by NO_3^- concentration and C consumption rates, and occurs only in the anoxic fraction of soils:

$$F_{\mathrm{denitr,p}} = \min\left(f(\mathrm{decomp}), f([\mathrm{NO_3^-}])\right) \mathrm{frac_{anox}}, \quad (11)$$

where $F_{\mathrm{denitr,p}}$ is the potential denitrification rate and $f(\mathrm{decomp})$ and $f([\mathrm{NO_3^-}])$ are the carbon- and nitrate- limited denitrification rate functions, respectively (Grosso et al., 2000). Because the modified CLM includes explicit treatment of soil biogeochemical vertical profiles, including diffusion of the trace gases O_2 and CH_4 (Riley et al., 2011), we base the calculation of anoxic fraction $\mathrm{frac_{anox}}$ on the anoxic microsite formulation of Arah and Vinten (1995):

$$\mathrm{frac_{anox}} = \exp\left(-a R_\psi^{-\alpha} V^{-\beta} C^{\gamma} [\theta + \chi\epsilon]^{\delta}\right), \quad (12)$$

where a, α, β, γ, and δ are constants (equal to 1.5×10^{-10}, 1.26, 0.6, 0.6, and 0.85, respectively), R_ψ is the radius of a typical pore space at moisture content ψ, V is the O_2 consumption rate, C is the O_2 concentration, θ is the water-filled pore space, χ is the ratio of diffusivity of oxygen in water to diffusivity of oxygen in air, and ϵ is the air-filled pore space (Arah and Vinten, 1995). These parameters are all calculated separately at each layer to define a profile of anoxic pore-space fraction in the soil. The Century nitrification/denitrification models used here also predict fluxes of N_2O via a "hole-in-the-pipe" approach (Firestone and Davidson, 1989); however, as the focus of this paper is on the coupling of the C and N cycles, details and calibration of the N_2O emissions will be addressed in future work.

2.4.2 Biological N fixation

In CLM4.0-CN, Biological N Fixation (BNF) is calculated as a saturating function of NPP (Thornton et al., 2007):

$$\mathrm{BNF} = 1.8\,(1 - \exp(-0.003\mathrm{NPP})), \quad (13)$$

where BNF is the N fixation rate (g N m^2 yr^{-1}) and NPP is the net primary production (g C m^2 yr^{-1}). There are multiple

problems with this approach: one is that the BNF input to the CLM4.0-CN mineral N pool is calculated using the prior year's NPP, and distributed evenly across the year, i.e., with no seasonal cycle. The effect of this formulation is that, at high latitudes, most of the N inputs occur when plants are inactive and are thus lost before they can be accessed by plants (because of the 2-day turnover of mineral N in the absence of plant demand; see Sect. 2.4.1). Another problem is that by linking the N inputs directly to the (N-limited) production, a destabilizing positive feedback loop is introduced into the model, such that increased (decreased) NPP leads to further N increases (decreases) and further increased (decreased) NPP. Lastly, observations show that N fixation is not simply related to NPP; for example, N fixation is higher in tropical savanna than tropical forest (Wang and Houlton, 2009). Here, we address the first problem only: we maintain the basic functional form or the BNF calculation, but add a seasonal cycle by using an exponentially lagged NPP function with a lag function of 7 days in order to introduce roughly the same seasonal cycle in BNF as in NPP. The other problems will be addressed in future work that will more mechanistically couple N inputs through N fixation to ecosystem N demand as impacted by the differing costs of fixing N in different environments (e.g. Houlton et al. (2008); Fisher et al. (2010))

2.4.3 Competition for N

Competition for mineral N substrates is based on the CLM-CN scheme in CLM4, in which the sole mineral N pool is shared between immobilization and plant uptake based on the relative demand of each process. In this study, we extend the competition, increasing the number of mineral N species (NO_3^- and NH_4^+), increasing the competing process demands, and adding a vertical dimension to the competition. In the revised scheme, there is competition for NH_4^+ by immobilization, plant uptake, and nitrification, and competition for NO_3^- by immobilization, plant uptake, and denitrification. When total demand exceeds supply, the allocation of a given mineral N pool to each competing processes is proportional to the N demand of that process. We assume that N competition is sequential, with competition for NH_4^+ first in each timestep and competition for NO_3^- second; there is high uncertainty as to which substrate is actually preferred by plants and microbes. For the distribution of N demand vertically, we assume that the microbial processes are limited by the amount of NO_3^- or NH_4^+ in the soil level where the demand is, while plants can access NH_4^+ and NO_3^- throughout the soil column. This competition scheme is implemented numerically by setting the initial plant NO_3^- and NH_4^+ demand at a given soil grid level to be equal to the product of the total plant N demand and the fraction of the total soil NO_3^- or NH_4^+ that is contained in that level. If, after competition at each level, excess N remains anywhere in the soil column, then plants are able to access it. This highly simplified representation does not allow consideration of the actual tradeoffs required of plants in allocating their resources to roots in order to meet their nutrient needs (Fisher et al., 2012; McMurtrie et al., 2012); future work will focus on a more mechanistic, vertically resolved allocation and uptake model that will better represent these tradeoffs.

2.5 Model equilibration

We assume that CLM4 is initially in approximate C equilibrium under pre-industrial (1850) conditions. To find this initial condition, we "spin up" the model, integrating it with atmospheric boundary conditions defined by a repeating 25-year atmospheric reanalysis dataset (1948–1972 of Qian et al. (2006)), and fixed, pre-industrial atmospheric CO_2 concentrations and N deposition.

However, because of the slow response times of the soil C and N pools, and the sensitivity of model productivity to N mineralized from these slow components, it is prohibitively computationally expensive to run the full model for the period of time required to achieve quasi-steady state in all of the configurations described here. Analytical and semi-analytical solutions can be found in certain soil models (Xia et al., 2012), but these have not been extended to the multi-level biogeochemistry described here. Thus, we base our model equilibration procedure on a modified form of the "accelerated decomposition" (AD) technique described by Thornton and Rosenbloom (2005) that is implemented in CLM4. The original formulation of this procedure accelerates each of the soil pools by a common factor (A). However, the use of a single A for all soil pools has two undesirable effects. The first is that by accelerating the faster soil pools, the turnover times for these faster pools can drop below the annual cycle, or even the diurnal cycle for the fast soil pools, which then affects the seasonal and diurnal distribution of N mineralization from these pools. Because there are strong seasonal and diurnal cycles in the modeled N demand, this change to the N supply leads to a steady state that differs significantly from the steady state of the full model. Because the degree of this disequilibrium increases with increasing A, the second effect is that this limits the ability to accelerate slower pools and requires a trade-off in A that minimizes the total time spent equilibrating the model in the accelerated-decomposition and full model modes. Since, unlike the CLM-CN, the modified CLM4.5 has a passive pool with turnover time > 100 yr, a much greater acceleration of this pool is needed to find steady state quickly; thus the standard accelerated decomposition method is impractical. However, a simple modification allows the technique to be significantly more efficient. This is is to accelerate each pool by a different degree, such that the slowest pools are accelerated more than the fast pools, and anything with turnover time less than one year is left unchanged. Thus, we define a vector of acceleration factors (A_i, Table 1) and adjust the level of accelerated decomposition during the initialization stage separately for each soil pool i such that the turnover times of

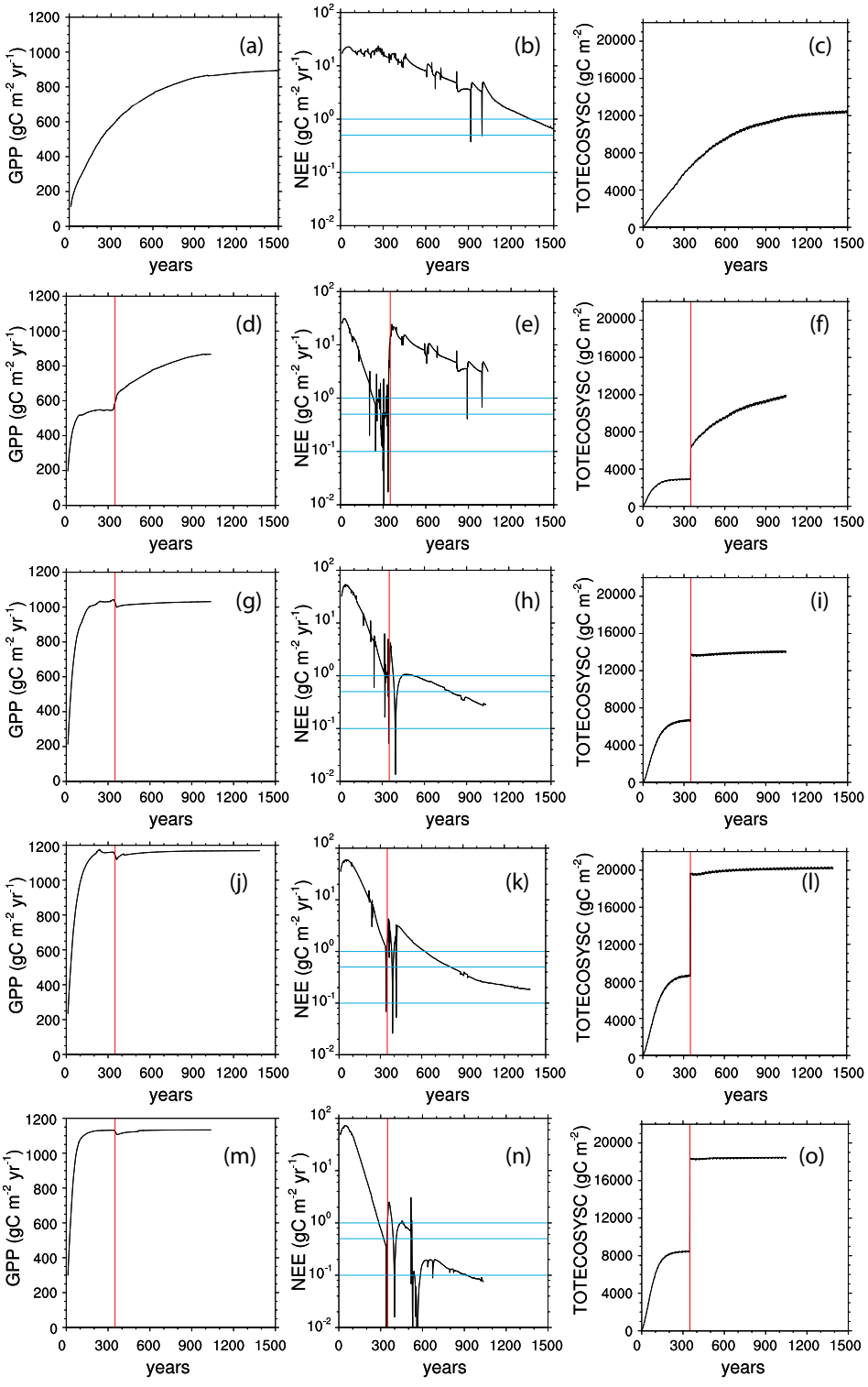

Fig. 4. A comparison of model equilibration time for different techniques, including the full model **(a–c)**, accelerated decomposition (AD) **(d–f)**, and modified accelerated decomposition **(g–o)**, for a single grid cell using multiple versions of model (a-i): CLM4.0 model, **(j–l)** single-level CLM4 with Century soil pools, **(m–o)** multi-level CLM4 with Century soil pools. Columns are: left **(a, d, g, j, m)** GPP; center **(b, e, h, k, n)** abs(log(NEE)), and right **(c, f, i, l, o)** total ecosystem carbon. Horizontal axis is time, in years, with the same scale for all simulations. Horizontal blue lines represent thresholds of abs(NEE) equal to 1, 0.5, and 0.1 $\mathrm{g\,C\,m^{-2}\,yr^{-1}}$. Vertical red lines represent the step in which the model is taken from spinup mode to normal mode.

the slowest pools are all collapsed onto an approximately annual timescale, which leads to a more accurate convergence to the native dynamics of the full model (Fig. 4). The vector A_i is then used at the end of the initialization procedure to multiply the carbon stocks to achieve quasi-steady state. We call this method "modified accelerated decomposition" (Modified-AD).

The inclusion of vertical transport also requires a modification of the vertical transport rates during the model initialization period. The essence of Modified-AD is that the equilibrium fluxes between any two pools remain approximately the same as in the base model, while the sizes of the equilibrium pools are reduced in order to allow them to be rapidly filled. We extend this idea to the vertical transport fluxes by multiplying the advection and diffusion coefficients of each soil pool i by the associated acceleration factor A_i; thus the vertical fluxes through the soils are also maintained so that they are equal to the base model despite the smaller pool size, which gives rise to the correct vertical profiles after exiting the Modified-AD mode. Lastly, an extension needs to be added to Modified-AD for the ^{14}C pools. Because the turnover time of the accelerated pools equals $1/A_i$ times the base model turnover times, the ^{14}C will be too young by the same factor. Thus we accelerate the radioactive decay in each soil pool i by the term A_i as well, leading to steady state pools with the same ^{14}C age distribution as in the base model.

2.6 Description of modeling experiments

We examine the sensitivity of several of the model's parameters and structural components, including: (1) varying soil decomposition cascades and associated turnover times in the default (CLM-CN) versus Century-based cascades; (2) vertical mixing rates; (3) explicit depth control on decomposition beyond moisture and temperature controls; (4) vertical profile of soil C and N inputs from above-ground and below-ground vegetation pools; (5) reactive N loss mechanisms in the default (CLM-CN) versus the Century-based model structures. In these sensitivity analyses, we compare profiles of predicted soil C content, ^{14}C age, soil and litter turnover times, and soil and litter C stocks with these sensitivity terms.

The baseline control for the global simulations is the CLM4.0-CN model. Because the biogeochemistry modifications described here were performed as part of a larger set of developments for a new version of CLM called CLM4.5, a second control simulation was performed using these other modifications, which include the following: modified photosynthesis calculations (Bonan et al., 2011, 2012), modified frozen soil hydrology (Swenson et al., 2012), and fractional snow cover (Swenson and Lawrence, 2012). We refer to this second control simulation as "CLM4.5-biogeophysics". Incremental changes to the biogeochemistry were then sequentially added on top of these changes: (1) modifying the SOM decomposition cascade, (2) adding the full vertical dimension to the soil biogeochemistry, and (3) replacing the CLM-CN mineral N submodel with resolved NO_3^-, NH_4^+, nitrification, and denitrification. We refer to this fully modified simulation as "CLM4.5-biogeophysics/biogeochemistry".

For all of these experiments, we force the model with meteorology from the Qian et al. (2006) bias-corrected reanalysis dataset. For the model years 1850–1947, we cycle atmospheric forcing from the period 1948–1972, and use the corresponding atmospheric data for the years 1948–2004. N deposition is prescribed following Lamarque et al. (2005), and CO_2 varies over the period following the observed ice core and atmospheric sampling record. Land-cover change and harvest follows the Hurtt et al. (2006) dataset.

3 Results and discussion

An important diagnostic of a model's biogeochemistry is the prediction of steady-state carbon stocks (Todd-Brown et al., 2013). Here we examine both the total SOM stocks (Fig. 5) and SOM ^{14}C values (Fig. 6). Maps of SOM carbon exist; here we compare them to the International Geosphere-Biosphere Programme (IGBP) Data and Information System (DIS) dataset (Global Soil Data Task Group, 2000), which is a global soil carbon map, and to the Northern Circumpolar Soil Carbon Database (NCSCD), (Tarnocai et al., 2007; Hugelius et al., 2013), which covers only the Northern circumpolar region. We include the NCSCD because it contains revised, higher, and more accurate estimates of the high-latitude soil C pool, which was poorly represented in earlier soil carbon maps. Global observational maps of soil ^{14}C do not exist, thus we use the global model-predicted soil ^{14}C distributions as a qualitative diagnostic, and also compare site-level observations to corresponding model grid cell predicted soil ^{14}C and C profiles. We also also histograms of soil C divided into three geographic bands (Fig. 7), in order to show the range of variation in the soil C predicted by the different versions of the model and by observations.

The base CLM4.0-CN Soil C (Fig. 5c), as well as the Soil C and ^{14}C of the CLM4.5-biogeophysics model (Fig. 5d and 6a), show a number of biases compared to the regional and global datasets. The CLM4.0-CN and CLM4.5-biogeophysics simulations show substantially less soil C than the observation-based maps. The age distribution of soil C in the base CLM4 biogeochemistry is very young – typical soil Δ^{14}C values are approx. -10 ‰, corresponding to a bulk turnover time of 80 yr. These Δ^{14}C values are much younger (i.e., more positive) than typically observed (Fig. 10). In addition, the CLM4.0-CN and CLM4.5-biogeophysics latitudinal gradients of soil C are very different from the observations: the observational databases show highest soil C in the high latitudes, while CLM4.0-CN and CLM4.5-biogeophysics show lowest soil C there. This change in soil C, particularly at high latitudes, is a result of changes to the

vegetation productivity due to soil N feedbacks from the revised denitrification model (Fig. 8).

3.1 Alternate C cascade

Using the single-layer model, a first comparison can be made between the CLM-CN and Century-based decomposition cascades (Fig. 5d and e). In a single-level model, the effect of the different decomposition cascades on the total C storage at equilibrium is modest. The effect of the changed decomposition pathway on fluxes is also modest, as the first-order control on these are the environmental parameters, which, for this exercise, we have left the same in both model versions. A large change can be seen, however, in SOM Δ^{14}C at preindustrial conditions (Fig. 6a and b). The new Century-based decomposition cascades lead to much older ^{14}C ages. This change follows from the dramatically faster turnover times in CLM-CN litter and SOM pools as compared to the Century pools. The faster litter decay predicted by the CN cascade is not supported by observations from long-term litterbag experiments (Bonan et al., 2013). Because pre-bomb SOM Δ^{14}C is much older than the -20 ‰ calculated using the CLM-CN pool structure, we use only the Century soil structure to examine the sensitivity of SOM Δ^{14}C profiles to transport and turnover processes.

3.2 Vertically resolved model

3.2.1 Site level vertical profiles of C and ^{14}C ages

Soil C age is a powerful constraint on soil turnover time and history. Its natural abundance is sensitive to long-term dynamics, such as slow turnover and transport processes, while its changes over the 20th century are sensitive to shorter-term dynamics (e.g. decadal turnover rates) through the incorporation of anthropogenic radiocarbon produced during bomb testing (Trumbore et al., 1989). We test the sensitivity of predicted soil ^{14}C on model parameters, and compare it with the soil ^{14}C profile data of Torn et al. (2002) collected at Voronazh, Russia. On advantage of this site is that it contains an archived soil sample from before the period of atmospheric weapons testing, which is sampled and compared to modern (1990) SOM. The site therefore has well-characterized ^{14}C profiles as functions of both natural abundance and after the addition of anthropogenic ^{14}C. Several other sites where ^{14}C profiles were reported in the literature are also shown in comparison with a baseline version of the model parameters in Fig. 10. For all comparisons in Figs. 9 and 10, we use the vertically resolved, Century-based decomposition cascade, and run the model offline forced by reanalysis (Qian et al., 2006) meteorology.

We first vary the transport rate of SOM C, examining the sensitivity of ^{14}C profiles to different specified advection (Fig. 9a), diffusion (Fig. 9b), and advection + diffusion (Fig. 9c) rates. The base SOM diffusivity here is $1\,\mathrm{cm^2\,yr^{-1}}$ and the base advection rate is $1\,\mathrm{cm\,yr^{-1}}$. For these experiments, z_τ, the direct e-folding depth control on SOM turnover, was set to infinity (thus no direct depth control on decomposition), and rooting profiles for C inputs were set to the default CLM root fractions. We were unable to match the slope of the depth-^{14}C relationship observed at any of the sites solely by varying the transport terms; this suggests that there was too much fresh carbon input at depth and/or that unresolved controls on turnover were slowing decomposition at depth.

Next, in Fig. 9d, we vary z_τ, the direct e-folding depth control on SOM turnover, applied to each of the soil and litter C pools. We vary this between infinity (i.e., no explicit depth dependence) and 0.4 m e-folding depth. The more rapid the increase in turnover time with depth, the steeper the slope in the pre-anthropogenic (solid line) ^{14}C curve with depth. With small z_τ, i.e., rapid slowing of decomposition with depth, the slope of the ^{14}C curve with depth becomes closer to the observed value. However, in contrast to the observations, a large increase in the SOM ^{14}C can still be observed with the bomb spike at depth, demonstrating that the main pulse of anthropogenic ^{14}C is limited to the top 10 cm at this site. An enrichment in observed ^{14}C is also seen in the 80–120 cm range, though this enrichment is likely due to inorganic C dynamics (Torn et al., 2002). This prediction shows that modeled inputs of fresh carbon are too large at depth compared to the observations.

In Fig. 9e, we vary the depth distribution of soil C inputs from roots. For each of these, we use a value of 0.5 m for z_τ, the imposed additional e-folding depth in soil C turnover. We consider three alternating model hypotheses to explain the mismatch between predictions and observations: (1) the base CLM root fractions, which follow a double exponential depth function (Zeng, 2001), (2) the single-exponential pft-specific root fraction function of depth (Jackson et al., 1996) and (3) a fixed e-folding depth. As noted above, the double exponential function for root fraction used in CLM leads to excessive C inputs at depth. The steepest gradient of ^{14}C with depth is found with shallow rooting inputs, with a 20 cm or smaller root C input profile e-folding depth required to be comparable to the slope in ^{14}C found at this site. In addition, the root input profile has a strong effect on the influence of bomb ^{14}C, with deeper root C inputs leading to deeper penetration of the bomb signal. However, even with shallow root inputs, the depth at which the change in soil ^{14}C is visible is slightly larger than in the observations. Thus the set of parameters that best matches the observed SOM ^{14}C profile are (1) slow mixing, (2) either a fixed e-folding depth or the Jackson et al. (1996) root fraction functions as C inputs, and (3) rapid increase in turnover time with depth.

In Fig. 10, we compare model predictions using a single, base set of parameters – 0.5 m z_τ (e-folding depth for soil turnover), Jackson et al. (1996) rooting depth for root C inputs, diffusivities of $1\,\mathrm{cm^2\,yr^{-1}}$ by bioturbation and $5\,\mathrm{cm^2\,yr^{-1}}$ for cryoturbation, and $0\,\mathrm{cm\,yr^{-1}}$ advection)

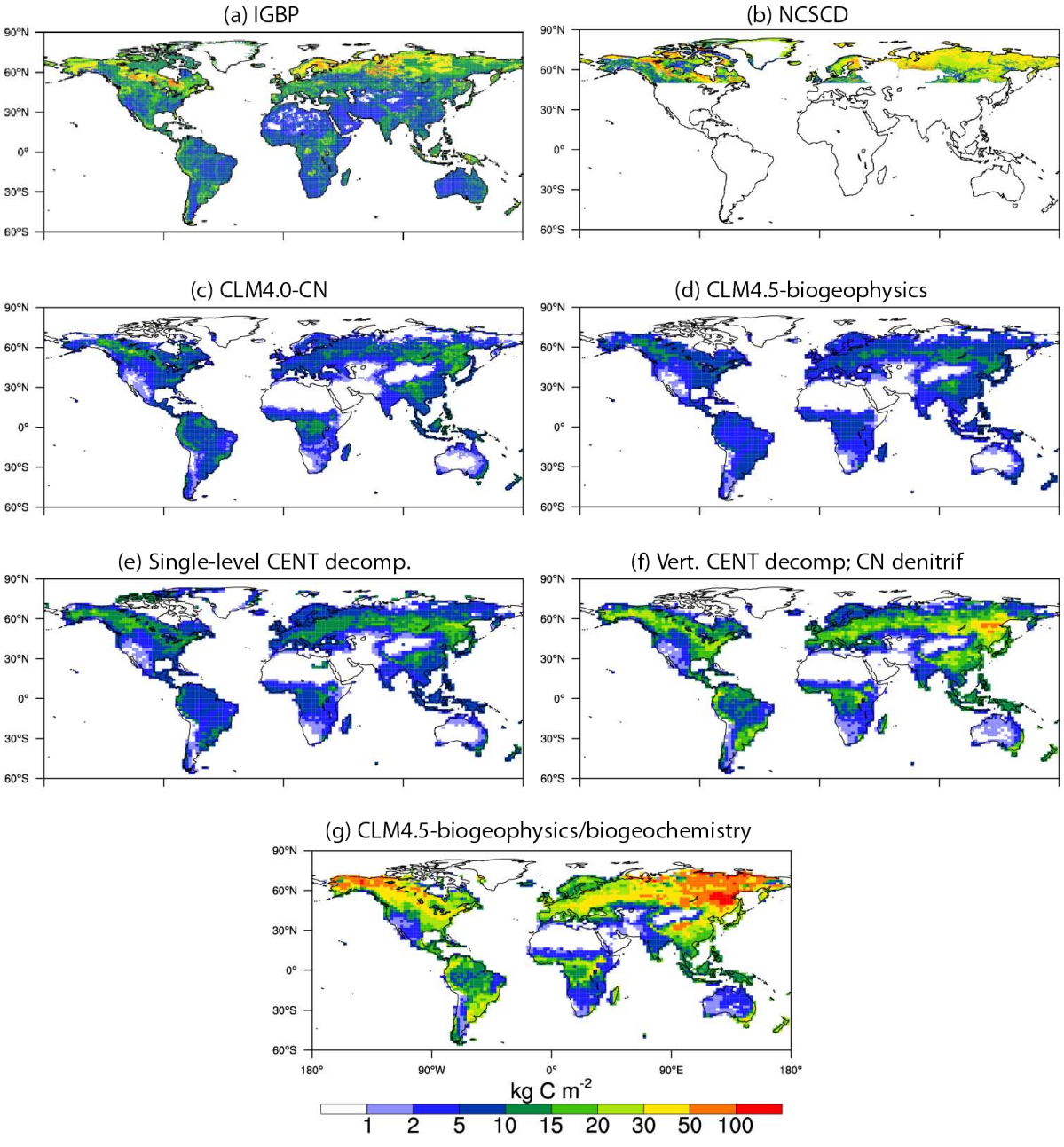

Fig. 5. Maps of soil C. **(a, b)** Observed soil C databases: **(a)** IGBP-DIS dataset (Global Soil Data Task Group, 2000); **(b)** NCSCD, (Tarnocai et al., 2007; Hugelius et al., 2013). **(c–g)** Modeled soil C for various cases: **(c)** base CLM4.0-CN; **(d)** CLM4.5-biogeophysics; **(e)** single-level biogeochemistry (BGC), Century-based decomposition; **(f)** multi-level BGC, Century-based decomposition, C N denitrification; **(g)** multi-level BGC, Century-based decomposition and nitrification/denitrification (CLM4.5-biogeophysics/biogeochemistry). For observations and multi-level model, data here is for upper 1 m of soil. Note quasi-logarithmic scale bar.

– to observations from sites where C and ^{14}C depth profiles have been measured and reported: Voronazh, Russia (Torn et al., 2002); Thule, Greenland (Horwath et al., 2008); Paragominas, Brazil (Trumbore et al., 1995); Mattole, California (Masiello et al., 2004); La Reunion, South Pacific (Basile-Doelsch et al., 2005); Harvard Forest, Massachusetts (Gaudinski et al., 2000); Gydansky, Western Siberia (Kaiser et al., 2007); and Judgeford, New Zealand; Riverbank, California; and Turlock Lake, California (Baisden and Parfitt, 2007).

These site-level comparisons show that C and ^{14}C profiles can be reasonably well simulated across a variety of ecosystems using the new vertically resolved Century-like C decomposition, imposed additional vertically resolved C

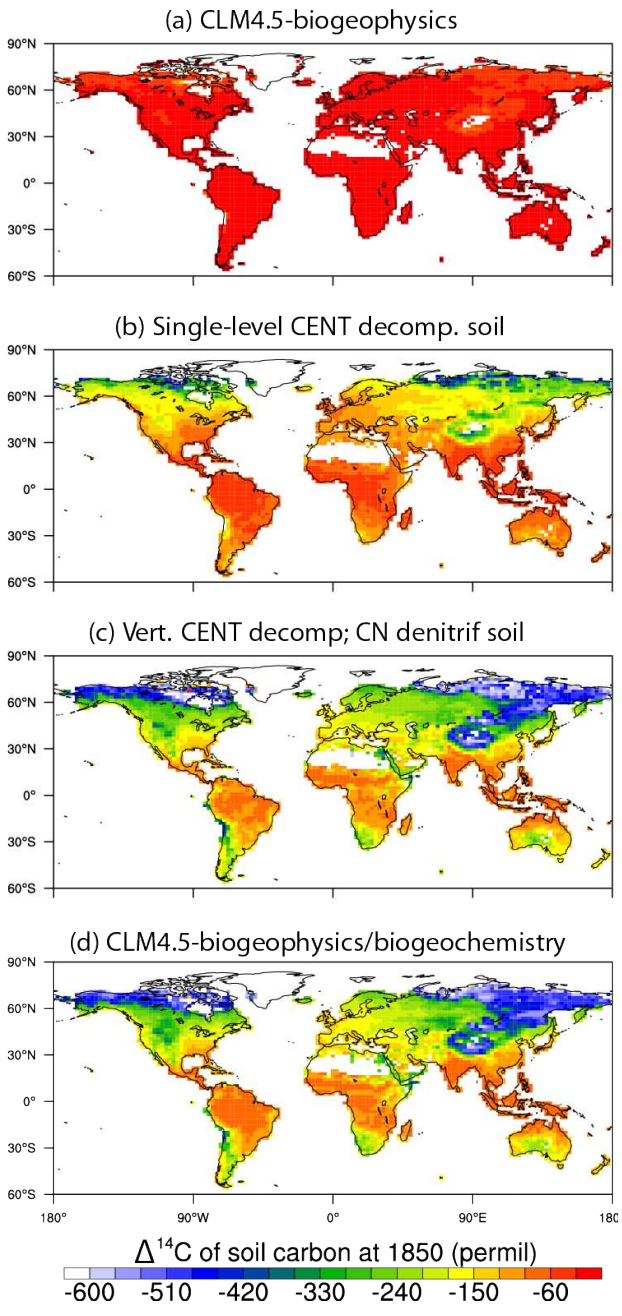

Fig. 6. Maps of SOM Δ ^{14}C for various cases: **(a)** base CLM4.5-biogeophysics; **(b)** single-level BGC, Century-based decomposition; **(c)** multi-level BGC, Century-based decomposition, CN denitrification; **(d)** multi-level BGC, Century-based decomposition and nitrification/denitrification (CLM4.5-biogeophysics/biogeochemistry). For multi-level model, results here are for upper 1 m of soil.

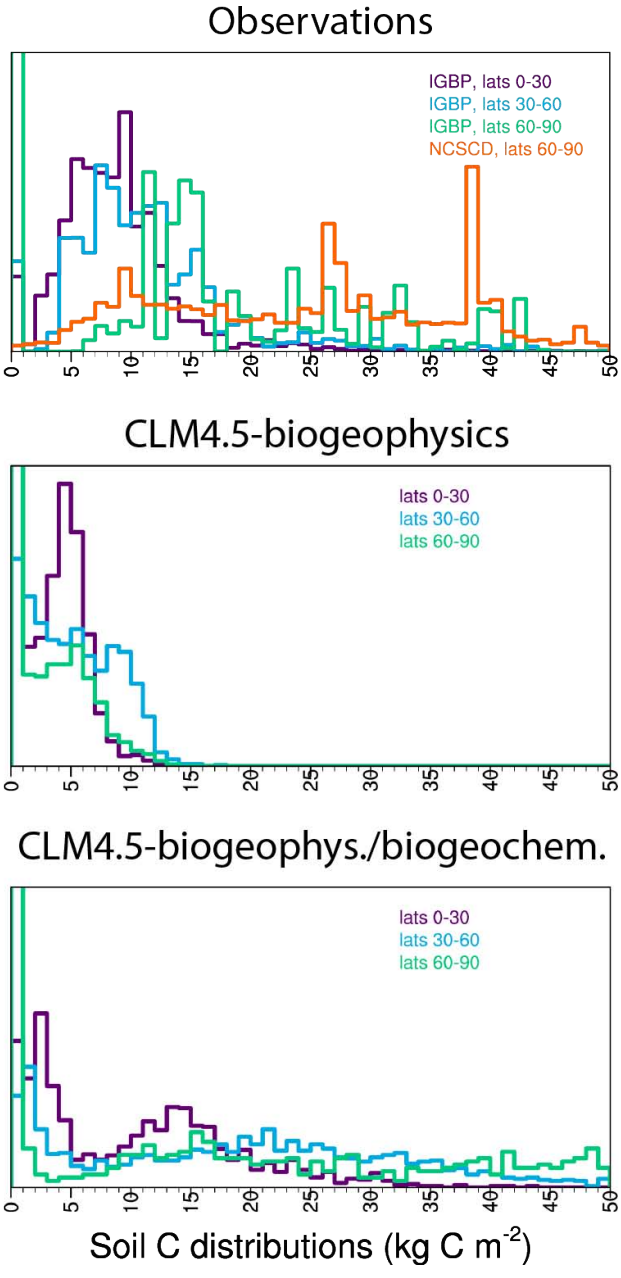

Fig. 7. Histograms of Soil C to 1 m for various model cases and for datasets

decomposition factor (z_τ), and baseline diffusive transport. The depth to which bomb carbon has been mixed is overestimated relative to the sites that include observations before and after the bomb signal. There does not appear to be a systematic bias in the total quantity of C at depth, except that many sites (e.g. Harvard Forest) have shallower soils than are simulated here; because soil depth is not known, our assumption here that soils are generally deep may lead to an overestimation of the quantity of deep soil C. The two tropical sites, Paragominas and La Reunion, show distinctly older carbon at depth than does the model. The control by mineral aggregates in the model is highly simplified, with the only direct effect being the textural control on the Century SOM cascade; thus, we are unable to reproduce the highly complex

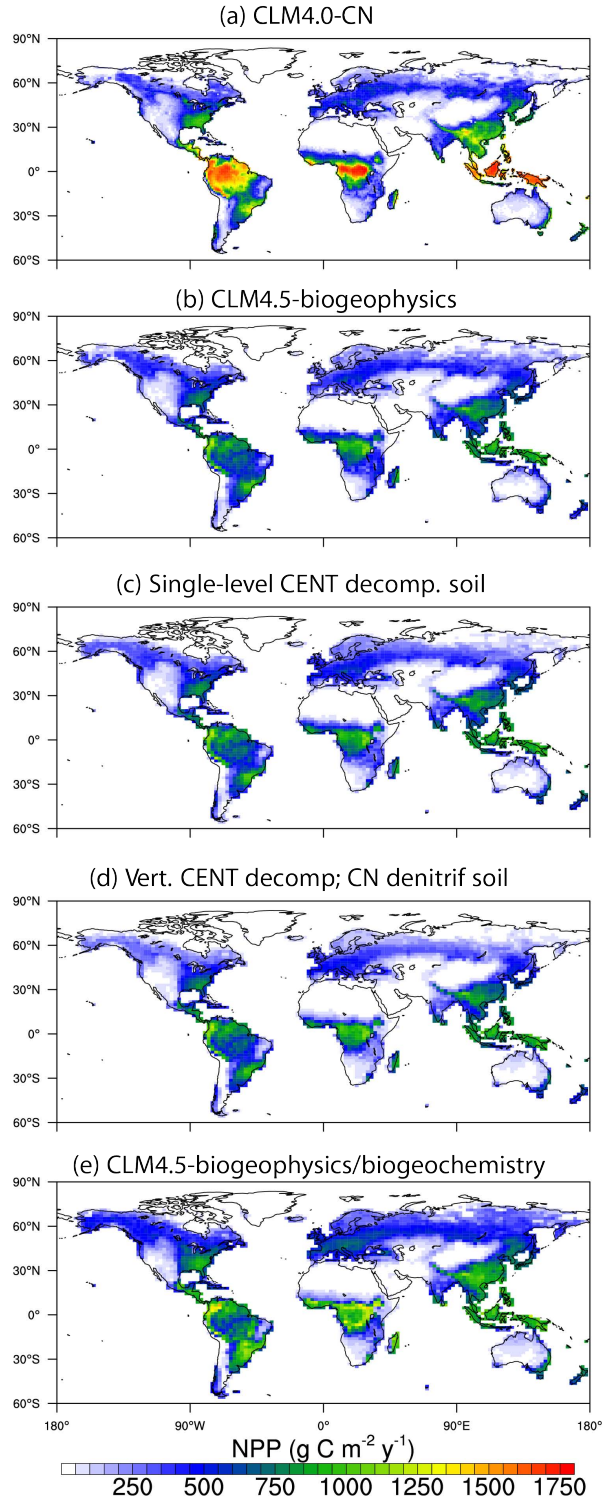

Fig. 8. Maps of mean annual NPP for each of the simulations. **(a)** CLM4.0-CN; **(b)** CLM4.5-biogeophysics; **(c)** single-level BGC, Century-based decomposition; **(d)** multi-level BGC, Century-based decomposition, CN denitrification; **(e)** multi-level BGC, Century-based decomposition and nitrification/denitrification (CLM4.5-biogeophysics/biogeochemistry).

relationships of the decadal to century turnover time pools observed at depth in natural soil profiles (Koarashi et al., 2012).

For these sites, the slope of the modeled ^{14}C age curves with depth is not compatible with turnover times that are invariant with depth beyond the environmental rate modifiers, even after inclusion of a passive C pool ($\tau \approx 500$–1000 yr) in the Century-based decomposition cascade, and with slow vertical transport. Therefore, we conclude that other factors act to reduce decomposition rates in the subsoil, beyond control by moisture, temperature, or intrinsic substrate lability. These factors could include: (1) pore-scale anoxia beyond the bulk anoxia limitation we apply here; (2) a strong control by the microbial community and the possible priming effects that may result from microbial population dynamics and lead to lesser microbial activity at depth; (3) other stabilization mechanisms such as SOM–mineral surface interactions, which may become more important with depth due to a smaller quantity of SOM relative to the total amount of mineral surface area. A similar explicit depth dependence to turnover time was found by Jenkinson and Coleman (2008). Future work to better understand the processes that control the vertical profiles of SOM turnover and stabilization is needed.

One possible explanation for the need to invoke a separate depth control on decomposition is that our treatment of anoxia and its effects on SOM turnover at depth may be oversimplified. The model assumes that respiration rates are not limited by oxygen unless the gross pore-space oxygen concentrations are insufficient to meet demands. An alternative hypothesis is that decomposition could be proportional to the volumetric fraction of oxic pore spaces (Arah and Vinten, 1995; Rappoldt and Crawford, 1999). However, when we calculate the oxic fraction following Arah and Vinten (1995) (Fig. 11e), in which the oxic fraction is controlled both by the O_2 consumption rate by respiration and the pore O_2 concentration, the result is a smaller oxic fraction at the surface than at depth, particularly in tropical soils, because of the much higher oxygen consumption rate in the soil surface than at depth; this mechanism would lead to the opposite effect in terms of the vertical profile of turnover times.

3.2.2 Global patterns of Decomposition and SOM stocks

Figure 11 shows latitude vs. depth profiles of the rate scalars used to limit decomposition, nitrification, and denitrification. The single-layer model uses the product of moisture and temperature scalars averaged over the top 30 cm of soil, whereas the vertically resolved model uses the product of the temperature, moisture, oxygen, and depth scalars at each model level. Temperature has only a weak vertical impact on predicted SOM turnover (Fig. 11a), since mean temperature does not vary strongly with depth; the limited vertical profile that is present is due to the concave-upwards curvature of the Q_{10}

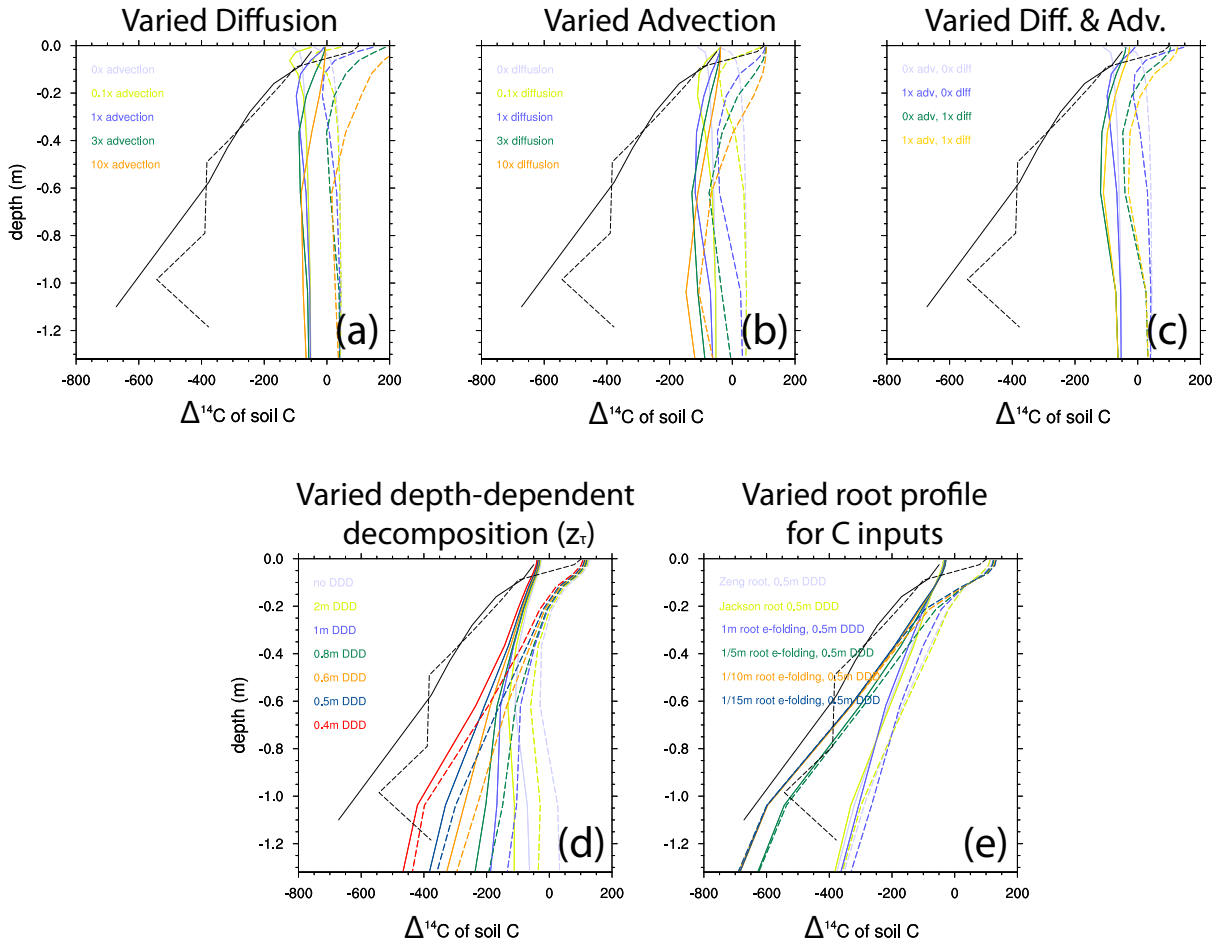

Fig. 9. Sensitivity of vertical profiles of soil $\Delta^{14}C$ to parameters at the Voronazh site. For all figures, solid line is archived (pre-bomb) soil $\Delta^{14}C$, and dashed line is modern (1990) $\Delta^{14}C$. **(a–c)** Response of soil $\Delta^{14}C$ to diffusion, advection, and combined advection plus diffusion. **(d)** Response of $\Delta^{14}C$ to depth control on soil turnover. **(e)** Response of $\Delta^{14}C$ to input profile of rooting depth.

formulation which implies that a larger amplitude at the surface translates to a slightly higher annual mean rate there (Sierra et al., 2011). The stronger vertical controls on predicted decomposition rates are due to moisture and oxygen availability. Moisture (Fig. 11b) limits decomposition at the surface at low and mid latitudes (because of surface drying), and at depth at high latitudes (because of freezing; see above for discussion of cryosuction effects on decomposition). Oxygen (Fig. 11c) limits decomposition at depth in low and high latitudes, but has little impact in the subtropics to midlatitudes because of relatively oxic conditions there. The aerobic fraction (Fig. 11e; $1 - \mathrm{frac}_{\mathrm{anox}}$), which is used to calculate where denitrification occurs, is low where respiration rates are high and soils are moist; this differs from the oxygen limitation for decomposition, which is merely based on supply and stoichiometric demand for oxygen.

When switching from the single-level model (Fig. 6b) to the fully vertically discretized form (Fig. 6c) while keeping the SOM decomposition cascade constant, a large change can be seen in the ^{14}C age in cold regions where permafrost soils exist. This old carbon at depth, which we model following Koven et al. (2009), is expected based on the profiles in Fig. 11 because decomposition is slowed greatly at depth in the permafrost. However, in CLM4, the effect on equilibrium soil C storage itself (Fig. 5e–f) is relatively modest at high latitudes. This small effect is because the excessively fast loss of N by denitrification in CLM4.0-CN leads to an extremely low productivity in these ecosystems. Therefore, even though the decomposition rates are very slow (since the C inputs are so low), the storage is still much smaller than observed. Amelioration of this anomalous N limitation, and its effects on the C storage, is discussed below.

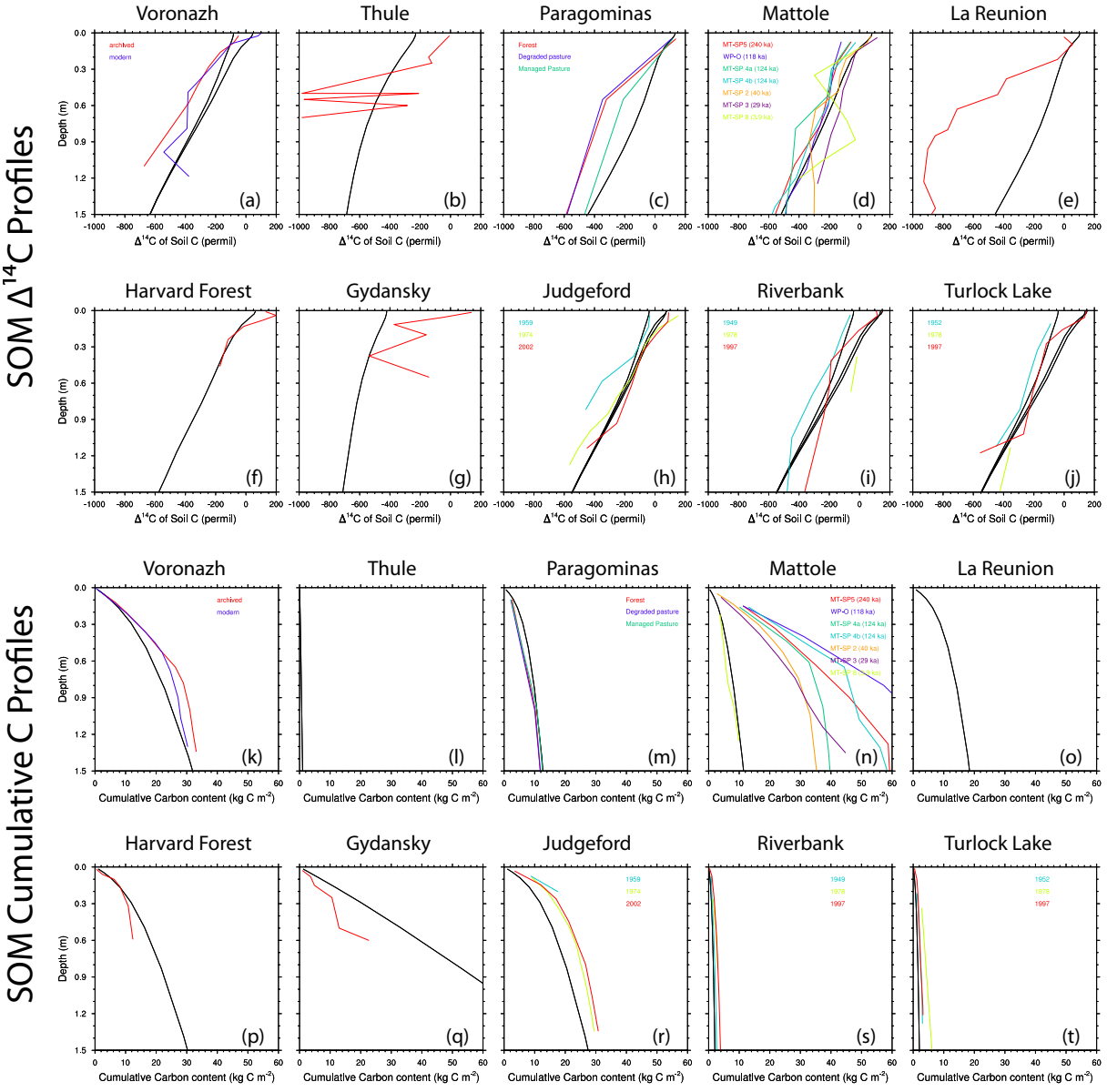

Fig. 10. Vertical profiles of soil C and Δ^{14}C for select sites: **(a, k)** Voronazh, Russia (Torn et al., 2002); **(b, l)** Thule, Greenland (Horwath et al., 2008); **(c, m)** Paragominas, Brazil (Trumbore et al., 1995); **(d, n)** Mattole, California (Masiello et al., 2004); **(e, o)** La Reunion, South Pacific (Basile-Doelsch et al., 2005); **(f, p)** Harvard Forest, Massachusetts (Gaudinski et al., 2000); **(g, q)** Gydansky, Western Siberia (Kaiser et al., 2007); and **(h, r)** Judgeford, New Zealand; **(i, s)** Riverbank, California; and **(j, t)** Turlock Lake, California (Baisden and Parfitt, 2007). For all figures, black line is model, and colored lines are observations. Some of the sites have multiple profiles, due to multiple soil ages (Mattole), multiple land-use types (Paragominas), and multiple sampling dates (Voronazh, Judgeford, Riverbank, and Turlock Lake). For those sites with multiple sampling dates, multiple model profiles are shown corresponding to the years of the soil sampling dates.

3.3 N cycle improvements

Updating the inorganic N cycle from the CLM4 scheme to the Century-based nitrification and denitrification schemes has a large effect on the productivity of the model, due to the tight coupling of the C and N cycles in CLM4. These large changes are particularly noticeable in areas where the growing season is short, because of how N losses are calculated in CLM4.0-CN. The default scheme uses a first-order decay with a time constant of two days via denitrification of mineral N not immediately used by plants or immobilization (Thornton and Rosenbloom, 2005), independent of the environmental conditions. Also, in CLM4.0-CN, N additions to the ecosystem via biological N fixation are aseasonal and calculated as a function of annual NPP (Thornton et al., 2007). The combined effects of these treatments in CLM4.0-CN

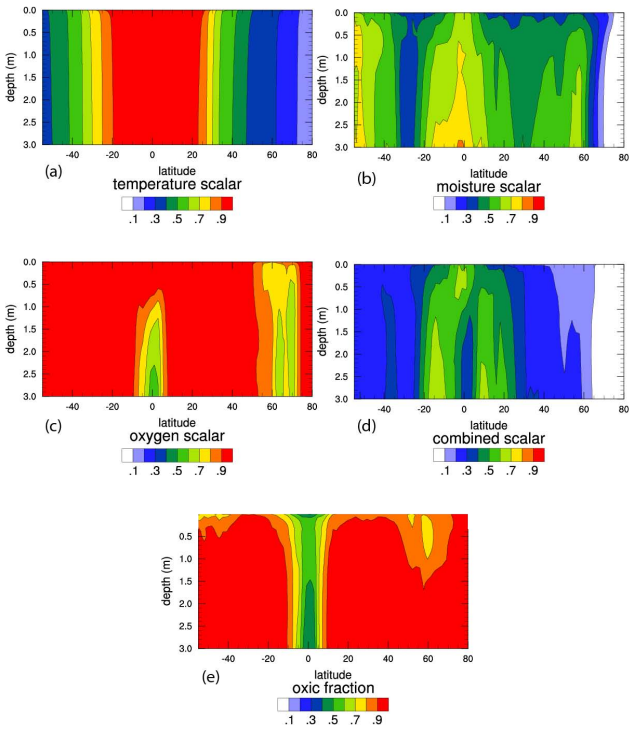

Fig. 11. Zonal- and annual-mean rate limiters for decomposition processes, as function of depth and latitude: **(a)** temperature scalar ($Q_{10} = 1.5$), **(b)** moisture scalar (Equation 5), **(c)** oxygen scalar, **(d)** combined scalar (not including explicit depth limitation) = temp × moist × ox, **(e)** oxic fraction, following Arah and Vinten (1995).

leads to an unexpected outcome at high latitudes, where, because the growing season is short, the majority of N inputs are lost before they are ever able to be incorporated into plant tissue; this creates a feedback loop that prevents establishment of vegetation. By linking gaseous N losses to environmental rate parameters in the Century scheme, and setting the N fixation seasonality so that it roughly follows the NPP seasonal cycle, the modified model allows N inputs to be used by plants, and therefore N, while still limiting, allows the model to break out of the near-zero productivity attractor present in CLM4.0-CN at high latitudes.

The impacts of relieving this unrealistic N limitation can be seen clearly in the predicted equilibrium C stocks in the new version of the model (Fig. 5g), in which the modified model builds up much higher C – in particular at high latitudes – as a result of the changed N cycle. The change in carbon can also be seen if we look at histograms of the model soil C concentrations (Fig. 7). The new model agrees considerably more than the CLM4.0-CN with observations of both the total quantities of soil C in the top meter of soil and the latitudinal distributions. However, several biases are still apparent. Soil C in arid and semiarid ecosystems (e.g., southwestern USA, Central Asia) is underestimated, most likely due to an underestimate of productivity in these regions. High latitude C stocks approach observed values, but C stocks in several regions that contain large peat deposits (e.g., Fennoscandia, Western Siberian Lowlands) are underestimated – as we expect since peatland formation processes are not currently included in the model.

Outside the high latitudes, the effect of changing the mineral N cycle is still large. The CLM4.0-CN mineral N cycle is essentially very open, in that losses are very high via the first-order 2-D denitrification term, such that N is highly limiting everywhere, even in tropical forest ecosystems where observations suggest that N is not a highly limiting resource (Bonan and Levis, 2010). One effect of the CLM4.5-biogeophysics changes is to reduce the intrinsic productivity of the carbon cycle; when combined with a more closed N cycle, the less strong denitrification loss reduces the overall strength of the N downregulation in the model.

Numbers for the global N source and sink budgets associated with the "slow" N cycle (processes other than the fast cycling of N between plants and SOM) in both the base and revised model versions are in Fig. 12. Galloway et al. (2004) report estimates for these source and sink terms for the pre-anthropogenic terrestrial biosphere: 120 Tg N yr^{-1} for BNF, 17.4 Tg N yr^{-1} Deposition, 69.8 Tg N yr^{-1} exported into rivers, and 98 Tg N yr^{-1} exported via denitrification. The baseline CLM4.0 has very small dissolved losses; these dissolved N losses are somewhat increased in the revised model but still far below the observational estimates. One reason for this underestimate is that, in the model, plants are still able to reduce the mineral N pools essentially to zero; current and future work on CLM is and will be focused on reducing the N uptake efficiency of plants at low mineral N concentrations (Thomas et al., 2013), and on linking the dissolved N and hydrologic pathways in order to remove this bias. The denitrification loss is comparable to the Galloway et al. (2004) budget, but above the 47 Tg N calculated by Bai et al. (2012); our denitrification results are highly uncertain.

3.4 Changes to global terrestrial C budget over the 20th century

The set of changes in the biogeophysics and biogeochemistry between CLM4.0 and CLM4.5 leads to large changes in the predicted terrestrial carbon budget over the second half of the 20th century (Figs. 13 and 14). CLM4.0-CN predicts a net loss of carbon from the terrestrial biosphere during the 20th century (Fig. 13c). Given that the observed airborne fraction was close to 0.5 and that oceanic uptake can only account for about half of the total C sink, this implies that the terrestrial biosphere was responsible for taking up approximately 25% of the anthropogenic carbon emissions (e.g., Le Quere et al., 2009). Thus the CLM4.0-CN simulation has the opposite sign to the inferred carbon balance over the late twentieth century.

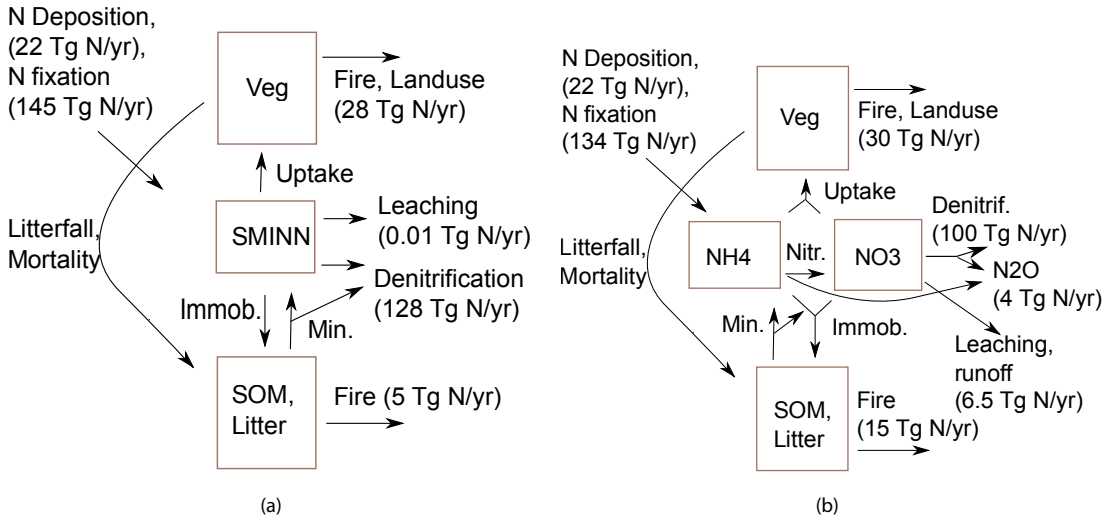

Fig. 12. Schematics of N cycle in base and updated versions of CLM4; numbers refer to the global mean slow N cycle source and sink terms for an 1850 control scenario.

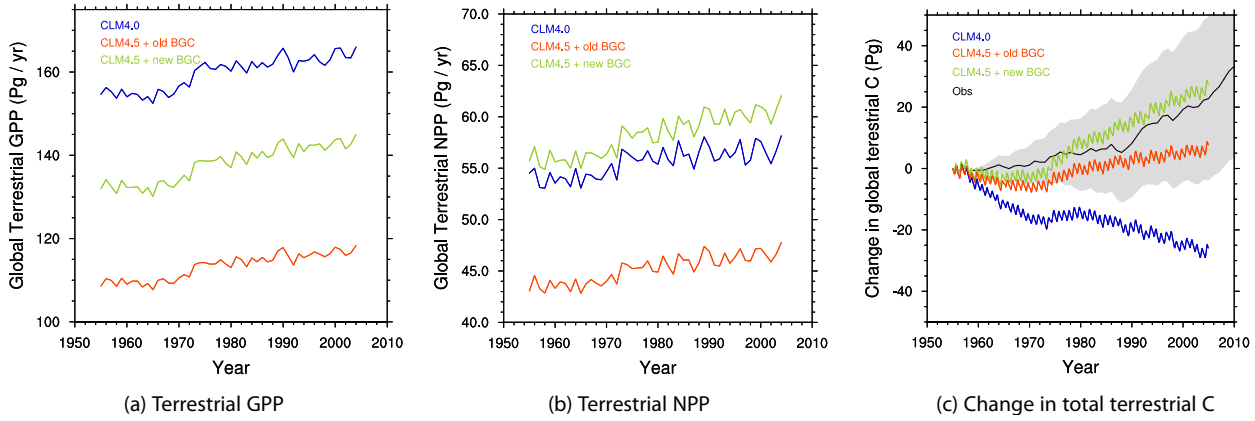

Fig. 13. Changes to global integrated carbon cycle quantities during a transient late-20th-century (1955–2005) model simulation forced by reanalysis meteorology and observed atmospheric CO_2 concentrations. **(a)** Gross primary productivity (GPP). **(b)** Net primary productivity (NPP). **(c)** Change from initial total terrestrial carbon stocks. Observations in **(c)** are the sum of the land sink and land-use fluxes from the Global Carbon Project (Le Quere et al., 2013), with errors calculated assuming that within each year the land error equals the root-sum-of-squares of the ocean and fossil fuel errors, and that errors are correlated interannually, so are additive in time. Model versions are the CLM4.0-CN, CLM4.5-biogeophysics, and CLM4.5-biogeophysics/biogeochemistry.

The set of changes between the CLM4.0-CN and CLM4.5-biogeophysics lead to sharply reduced terrestrial gross primary productivity (GPP), from $\approx 160\,\mathrm{Pg\,C\,yr^{-1}}$ to $\approx 110\,\mathrm{Pg\,C\,yr^{-1}}$ (Fig. 13a). Most of this reduction occurs in the tropical forests, which in CLM4.0-CN have unrealistically high GPP values (Beer et al., 2010), as a result of reduced photosynthesis following the revised calculations described in Bonan et al. (2011, 2012). Because tropical forests in CLM have relatively low carbon use efficiency (defined as the ratio of NPP to GPP), the reduced GPP in the tropical forests leads to a proportionally smaller decrease in the global NPP (Fig. 13b). However, because the overall limitation by nitrogen is weakened due to the intrinsically lower photosynthetic uptake, the biosphere is more responsive to the increased temperature and CO_2 concentrations, leading to a larger net uptake of carbon overall, which shifts the biosphere from a source to a weak sink of carbon (Fig. 13c). This shift can be seen by looking at the latitudinal profiles of the change in C pools (Fig. 14a–b), in which the tropical vegetation transient increase is higher in the CLM4.5-biogeophysics simulation than the CLM4.0-CN simulation. There is larger storage in the litter and soil pools as well, despite the fact that the shift does not change the turnover times to these pools.

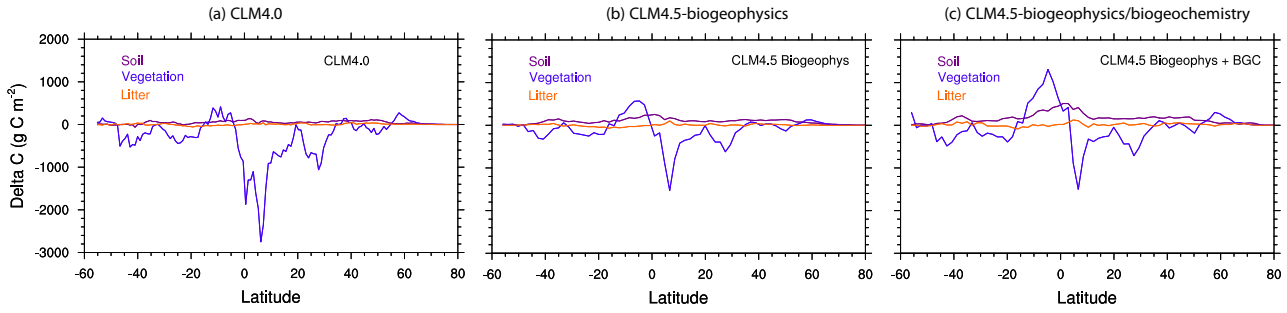

Fig. 14. Change over transient late-20th-century (2005–1955) model simulations in terrestrial C pools, as a function of latitude, for three models: **(a)** CLM4.0-CN, **(b)** CLM4.5-biogeophysics, and **(c)** CLM4.5-biogeophysics/biogeochemistry.

The set of soil biogeochemistry changes described here, between the CLM4.5-biogeophysics and CLM4.5-biogeophysics/biogeochemistry simulations, leads to an increase in much of the global GPP total (Fig. 13a). This increase can mainly be attributed to the revised soil mineral N cycle, which, by lengthening the residence time of the mineral N pools, allows N to be more efficiently retained and recycled by the ecosystem; therefore, less overall downregulation by nitrogen limitation occurs. Because this reduction of N downregulation effect is higher at high latitudes (where CLM simulates a relatively high carbon use efficiency), the increase in NPP from the CLM4.5-biogeophysics to the CLM4.5-biogeophysics/biogeochemistry simulations is proportionally larger than the GPP increase, bringing the global total almost back to the CLM4.0-CN value (Fig. 13b). The effect on total ecosystem carbon storage is again to increase the land uptake during the 20th century through a combination of reducing the N downregulation and increasing the turnover time of the decomposing carbon pools. The latitude profiles of transient storage show this effect, with further increases to tropical vegetation as well as increases to the soil and litter pools following the change to longer-turnover decomposition structure.

4 Conclusions

We describe a set of modifications to the biogeochemistry of CLM4. These include: (1) an option to use alternate soil and litter decomposition cascades, (2) the addition of a vertical profile to soil and litter biogeochemical dynamics, (3) changes to the model's mineral N cycle, including separate treatment of NO_3^- and NH_4^+, (4) the addition of a ^{14}C tracer to all model C pools for tracking the natural abundance and uptake of anthropogenic ^{14}C throughout the model, and (5) a revised model equilibration procedure.

Comparison between site-specific model simulations and observations suggest several parameter choices for the vertical soil model. The young ^{14}C ages in the CLM4.0-CN decomposition cascade are incompatible with observations; thus we proceed using the alternate, Century-based decomposition cascade. Comparison between model-predicted and observed ^{14}C vertical profiles suggests that turnover times are increased at depth beyond what is predicted using only the environmental rate modifiers of moisture, temperature, and oxygen, suggesting that additional, unresolved limitations of microbial activity or other SOM stabilization processes are important in slowing decomposition at depth. Overall root C inputs are low at depth, suggesting that even if deeper roots are involved in moisture uptake, deeper roots may not be proportionally represented in C inputs to the soil.

These changes have a substantial impact on the equilibrium C stocks and dynamical response of the model to 20th century global change, including a large increase in the total soil C stocks and a shift in C stocks from low to high latitudes, both of which bring the model into closer agreement with observations. In addition, the dynamic response in global C uptake over the 20th century is brought into better agreement with the historical record, as the modeled land biosphere is shifted from a C source to a sink, through a combination of reduced N downregulation and shifting the turnover of decomposing carbon to longer timescales.

Acknowledgements. This research was supported by the Director, Office of Science, Office of Biological and Environmental Research of the US Department of Energy under Contract No. DE-AC02-05CH11231 as part of their Climate and Earth System Modeling Program and used resources of the National Energy Research Scientific Computing Center (NERSC), also supported by the Office of Science of the US Department of Energy under Contract No. DE-AC02-05CH11231. Thanks to Abby Swann for discussion about improving model spinup performance, and to Peter Thornton for several discussions about the CLM-CN model. Thanks to Chris Jones, Philippe Ciais, and an anonymous reviewer for comments that improved the manuscript.

Edited by: P. Stoy

References

Andrén, O. and Paustian, K.: Barley straw decomposition in the field: a comparison of models, Ecology, 68, 1190–1200, 1987.

Arah, J. and Vinten, A.: Simplified models of anoxia and denitrification in aggregated and simple-structured soils, Eur. J. Soil Sci., 46, 507–517, 1995.

Arora, V. K., Boer, G. J., Friedlingstein, P., Eby, M., Jones, C. D., Christian, J. R., Bonan, G., Bopp, L., Brovkin, V., Cadule, P., Hajima, T., Ilyina, T., Lindsay, K., Tjiputra, J. F., and Wu, T.: Carbon-concentration and carbon-climate feedbacks in CMIP5 Earth system models, J. Climate, doi:10.1175/JCLI-D-12-00494.1, 2013.

Bai, E., Houlton, B. Z., and Wang, Y. P.: Isotopic identification of nitrogen hotspots across natural terrestrial ecosystems, Biogeosciences, 9, 3287–3304, doi:10.5194/bg-9-3287-2012, 2012.

Baisden, W. T. and Parfitt, R. L.: Bomb C-14 enrichment indicates decadal C pool in deep soil?, Biogeochemistry, 85, 59–68, doi:10.1007/s10533-007-9101-7, 2007.

Baisden, W. T., Amundson, R., Brenner, D. L., Cook, A. C., Kendall, C., and Harden, J. W.: A multiisotope C and N modeling analysis of soil organic matter turnover and transport as a function of soil depth in a California annual grassland soil chronosequence, Global Biogeochem. Cy., 16, 1135, doi:10.1029/2001GB001823, 2002.

Basile-Doelsch, I., Amundson, R., Stone, W., Masiello, C., Bottero, J., Colin, F., Masin, F., Borschneck, D., and Meunier, J.: Mineralogical control of organic carbon dynamics in a volcanic ash soil on La Reunion, Eur. J. Soil Sci., 56, 689–703, doi:10.1111/j.1365-2389.2005.00703.x, 2005.

Beer, C., Reichstein, M., Tomelleri, E., Ciais, P., Jung, M., Carvalhais, N., Rodenbeck, C., Arain, M. A., Baldocchi, D., Bonan, G. B., Bondeau, A., Cescatti, A., Lasslop, G., Lindroth, A., Lomas, M., Luyssaert, S., Margolis, H., Oleson, K. W., Roupsard, O., Veenendaal, E., Viovy, N., Williams, C., Woodward, F. I., and Papale, D.: Terrestrial Gross Carbon Dioxide Uptake: Global Distribution and Covariation with Climate, Science, 329, 834–838, 2010.

Bonan, G. B. and Levis, S.: Quantifying carbon-nitrogen feedbacks in the Community Land Model (CLM4), Geophys. Res. Lett., 37, L07401, doi:10.1029/2010GL042430, 2010.

Bonan, G. B., Lawrence, P. J., Oleson, K. W., Levis, S., Jung, M., Reichstein, M., Lawrence, D. M., and Swenson, S. C.: Global FLUXNET diagnostic models improve canopy processes in the Community Land Model (CLM4), J. Geophys. Res.-Biogeo., 116, G02014, doi:10.1029/2010JG001593, 2011.

Bonan, G. B., Oleson, K. W., Fisher, R. A., Lasslop, G., and Reichstein, M.: Reconciling leaf physiological traits and canopy flux data: Use of the TRY and FLUXNET databases in the Community Land Model version 4, J. Geophys. Res., 117, G02026, doi:10.1029/2011JG001913, 2012.

Bonan, G. B., Hartman, M. D., Parton, W. J., and Wieder, W. R.: Evaluating litter decomposition in earth system models with long-term litterbag experiments: an example using the Community Land Model version 4 (CLM4), Glob. Change Biol., 19, 957–974, doi:10.1111/gcb.12031, 2013.

Bosatta, E. and Agren, G.: Dynamics Of Carbon And Nitrogen In The Organic-Matter Of The Soil – A Generic Theory, Am. Nat., 138, 227–245, 1991.

Braakhekke, M. C., Beer, C., Hoosbeek, M. R., Reichstein, M., Kruijt, B., Schrumpf, M., and Kabat, P.: SOMPROF: A vertically explicit soil organic matter model, Ecol. Model., 222, 1712–1730, 2011.

Bruun, S., Christensen, B., Thomsen, I., Jensen, E., and Jensen, L.: Modeling vertical movement of organic matter in a soil incubated for 41 years with 14C labeled straw, Soil Biol. Biochem., 39, 368–371, 2007.

Davidson, E. and Janssens, I.: Temperature sensitivity of soil carbon decomposition and feedbacks to climate change, Nature, 440, 165–173, doi:10.1038/nature04514, 2006.

Elzein, A. and Balesdent, J.: Mechanistic simulation of vertical distribution of carbon concentrations and residence times in soils, Soil Sci. Soc. Am. J., 59, 1328, doi:10.2136/sssaj1995.03615995005900050019x, 1995.

Firestone, M. and Davidson, E.: Exchange of Trace Gases between Terrestrial Ecosystems and the Atmosphere, chap. Microbiological basis of NO and nitrous oxide production and consumption in soil, 7–21, John Wiley and Sons, 1989.

Fisher, J. B., Sitch, S., Malhi, Y., Fisher, R. A., Huntingford, C., and Tan, S. Y.: Carbon cost of plant nitrogen acquisition: A mechanistic, globally applicable model of plant nitrogen uptake, retranslocation, and fixation, Global Biogeochem. Cy., 24, GB1014, doi:10.1029/2009GB003621, 2010.

Fisher, J. B., Badgley, G., and Blyth, E.: Global nutrient limitation in terrestrial vegetation, Global Biogeochem. Cy., 26, GB3007, doi:10.1029/2011GB004252, 2012.

Friedlingstein, P., Cox, P., Betts, R., Bopp, L., von Bloh, W., Brovkin, V., Cadule, P., Doney, S., Eby, M., Fung, I., Bala, G., John, J., Jones, C., Joos, F., Kato, T., Kawamiya, M., Knorr, W., Lindsay, K., Matthews, H. D., Raddatz, T., Rayner, P., Reick, C., Roeckner, E., Schnitzler, K. G., Schnur, R., Strassmann, K., Weaver, A. J., Yoshikawa, C., and Zeng, N.: Climate–Carbon Cycle Feedback Analysis: Results from the C4MIP Model Intercomparison, J. Climate, 19, 3337–3353, 2006.

Frolking, S., Roulet, N. T., Moore, T. R., Richard, P. J. H., Lavoie, M., and Muller, S. D.: Modeling Northern Peatland Decomposition and Peat Accumulation, Ecosystems, 4, 479–498, doi:10.1007/s10021-001-0105-1, 2001.

Galloway, J., Dentener, F., Capone, D., Boyer, E., Howarth, R., Seitzinger, S., Asner, G., Cleveland, C., Green, P., Holland, E., Karl, D., Michaels, A., Porter, J., Townsend, A., and Vorosmarty, C.: Nitrogen cycles: past, present, and future, Biogeochemistry, 70, 153–226, 2004.

Gaudinski, J., Trumbore, S., Davidson, E., and Zheng, S.: Soil carbon cycling in a temperate forest: radiocarbon-based estimates of residence times, sequestration rates and partitioning of fluxes, Biogeochemistry, 51, 33–69, 2000.

Global Soil Data Task Group: Global Gridded Surfaces of Selected Soil Characteristics (IGBP-DIS), Data set, International Geosphere-Biosphere Programme – Data and Information System, available at: http://www.daac.ornl.gov from Oak Ridge National Laboratory Distributed Active Archive Center, Oak Ridge, Tennessee, USA, 2000.

Grosso, S. J. D., Parton, W. J., Mosier, A. R., Ojima, D. S., Kulmala, A. E., and Phongpan, S.: General model for N_2O and N_2 gas emissions from soils due to dentrification, Global Biogeochem. Cy., 14, 1045–1060, doi:10.1029/1999GB001225, 2000.

Heimsath, A., Chappell, J., Spooner, N., and Questiaux, D.: Creeping soil, Geology, 30, 111–114, 2002.

Horwath, J. L., Sletten, R. S., Hagedorn, B., and Hallet, B.: Spatial and temporal distribution of soil organic carbon in nonsorted striped patterned ground of the High Arctic, J. Geophys. Res.-Biogeo., 113, G03S07, doi:10.1029/2007JG000511, 2008.

Houlton, B. Z., Wang, Y. P., Vitousek, P. M., and Field, C. B.: A unifying framework for dinitrogen fixation in the terrestrial biosphere, Nature, 454, 327–U34, doi:10.1038/nature07028, 2008.

Hugelius, G., Tarnocai, C., Broll, G., Canadell, J. G., Kuhry, P., and Swanson, D. K.: The Northern Circumpolar Soil Carbon Database: spatially distributed datasets of soil coverage and soil carbon storage in the northern permafrost regions, Earth Syst. Sci. Data, 5, 3–13, doi:10.5194/essd-5-3-2013, 2013.

Hurtt, G. C., Frolking, S., Fearon, M. G., Moore, B., Shevliakova, E., Malyshev, S., Pacala, S. W., and Houghton, R. A.: The underpinnings of land-use history: three centuries of global gridded land-use transitions, wood-harvest activity, and resulting secondary lands, Glob. Change Biol., 12, 1208–1229, doi:10.1111/j.1365-2486.2006.01150.x, 2006.

Jackson, R. B., Canadell, J., Ehleringer, J. R., Mooney, H. A., Sala, O. E., and Schulze, E. D.: A global analysis of root distributions for terrestrial biomes, Oecologia, 108, 389–411, doi:10.1007/BF00333714, 1996.

Jarvis, N. J., Taylor, A., Larsbo, M., Etana, A., and Rosen, K.: Modelling the effects of bioturbation on the re-distribution of ^{137}Cs in an undisturbed grassland soil, Eur. J. Soil Sci., 61, 24–34, doi:10.1111/j.1365-2389.2009.01209.x, 2010.

Jenkinson, D. and Coleman, K.: The turnover of organic carbon in subsoils. Part 2. Modelling carbon turnover, Eur. J. Soil Sci., 59, 400–413, 2008.

Jenkinson, D., Adams, D., and Wild, A.: Model Estimates Of CO_2 Emissions from soil in response to global Warming, Nature, 351, 304–306, 1991.

Jenkinson, D. S., Poulton, P. R., and Bryant, C.: The turnover of organic carbon in subsoils. Part 1. Natural and bomb radiocarbon in soil profiles from the Rothamsted long-term field experiments, Eur. J. Soil Sci., 59, 391–U13, doi:10.1111/j.1365-2389.2008.01025.x, 2008.

Jones, C., Cox, P., and Huntingford, C.: Uncertainty in climate-carbon-cycle projections associated with the sensitivity of soil respiration to temperature, Tellus B, 55, 642–648, 2003.

Joslin, J. D., Gaudinski, J. B., Torn, M. S., Riley, W. J., and Hanson, P. J.: Fine-root turnover patterns and their relationship to root diameter and soil depth in a C-14-labeled hardwood forest, New Phytol., 172, 523–535, doi:10.1111/j.1469-8137.2006.01847.x, 2006.

Kaiser, C., Meyer, H., Biasi, C., Rusalimova, O., Barsukov, P., and Richter, A.: Conservation of soil organic matter through cryoturbation in arctic soils in Siberia, J. Geophys. Res.-Biogeo., 112, G02017, doi:10.1029/2006JG000258, 2007.

Kaste, J., Heimsath, A., and Bostick, B.: Short-term soil mixing quantified with fallout radionuclides, Geology, 35, 243, doi:10.1130/G23355A.1, 2007.

Koarashi, J., Hockaday, W. C., Masiello, C. A., and Trumbore, S. E.: Dynamics of decadally cycling carbon in subsurface soils, J. Geophys. Res.-Biogeo., 117, G03033, doi:10.1029/2012JG002034, 2012.

Koven, C., Friedlingstein, P., Ciais, P., Khvorostyanov, D., Krinner, G., and Tarnocai, C.: On the formation of high-latitude soil carbon stocks: The effects of cryoturbation and insulation by organic matter in a land surface model, Geophys. Res. Lett., 36, L21501, doi:10.1029/2009GL040150, 2009.

Koven, C. D., Ringeval, B., Friedlingstein, P., Ciais, P., Cadule, P., Khvorostyanov, D., Krinner, G., and Tarnocai, C.: Permafrost carbon-climate feedbacks accelerate global warming, P. Natl. Acad. Sci., 108, 14769–14774, doi:10.1073/pnas.1103910108, 2011.

Lamarque, J. F., Kiehl, J. T., Brasseur, G. P., Butler, T., Cameron-Smith, P., Collins, W. D., Collins, W. J., Granier, C., Hauglustaine, D., Hess, P. G., Holland, E. A., Horowitz, L., Lawrence, M. G., McKenna, D., Merilees, P., Prather, M. J., Rasch, P. J., Rotman, D., Shindell, D., and Thornton, P.: Assessing future nitrogen deposition and carbon cycle feedback using a multimodel approach: Analysis of nitrogen deposition, J. Geophys. Res.-Atmos., 110, D19303, doi:10.1029/2005JD005825, 2005.

Lawrence, D. M., Slater, A. G., Romanovsky, V. E., and Nicolsky, D. J.: Sensitivity of a model projection of near-surface permafrost degradation to soil column depth and representation of soil organic matter, J. Geophys. Res., 113, F02011, doi:10.1029/2007JF000883, 2008.

Lawrence, D. M., Oleson, K. W., Flanner, M. G., Thornton, P. E., Swenson, S. C., Lawrence, P. J., Zeng, X., Yang, Z.-L., Levis, S., Sakaguchi, K., Bonan, G. B., and Slater, A. G.: Parameterization Improvements and Functional and Structural Advances in Version 4 of the Community Land Model, J. Adv. Model. Earth Syst., 3, M03001, doi:10.1029/2011MS000045, 2011.

Le Quere, C., Raupach, M. R., Canadell, J. G., and Marland, G., Le Quéré, C., Raupach, M. R., Canadell, J. G., Marland, G., Bopp, L., Ciais, P., Conway, T. J., Doney, S. C., Feely, R. A., Foster, P., Friedlingstein, P., Gurney, K., Houghton, R. A., House, J. I., Huntingford, C., Levy, P. E., Lomas, M. R., Majkut, J., Metzl, N., Ometto, J. P., Peters, G. P., Prentice, I. C., Randerson, J. T., Running, S. W., Sarmiento, J. L., Schuster, U., Sitch, S., Takahashi, T., Viovy, N., van der Werf, G. R., and Woodward, I. F.: Trends in the sources and sinks of carbon dioxide, Nat. Geosci., 2, 831–836, doi:10.1038/ngeo689, 2009.

Le Quere, C., Andres, R. J., Boden, T., Conway, T., Houghton, R. A., House, J. I., Marland, G., Peters, G. P., van der Werf, G. R., Ahlström, A., Andrew, R. M., Bopp, L., Canadell, J. G., Ciais, P., Doney, S. C., Enright, C., Friedlingstein, P., Huntingford, C., Jain, A. K., Jourdain, C., Kato, E., Keeling, R. F., Klein Goldewijk, K., Levis, S., Levy, P., Lomas, M., Poulter, B., Raupach, M. R., Schwinger, J., Sitch, S., Stocker, B. D., Viovy, N., Zaehle, S., and Zeng, N.: The global carbon budget 1959–2011, Earth Syst. Sci. Data, 5, 165–185, doi:10.5194/essd-5-165-2013, 2013.

Levin, I. and Kromer, B.: The tropospheric 14CO2 level in mid-latitudes of the Northern Hemisphere (1959–2003), Radiocarbon, 46, 1261–1272, 2004.

Mahecha, M. D., Reichstein, M., Carvalhais, N., Lasslop, G., Lange, H., Seneviratne, S. I., Vargas, R., Ammann, C., Arain, M. A., Cescatti, A., Janssens, I. A., Migliavacca, M., Montagnani, L., and Richardson, A. D.: Global Convergence in the Temperature Sensitivity of Respiration at Ecosystem Level, Science, 329, 838–840, 2010.

Manning, M. and Melhuish, W.: Trends: A Compendium of Data on Global Change, Carbon Dioxide Information Analysis Center,

chap. Atmospheric ^{14}C record from Wellington, Oak Ridge National Laboratory, US Department of Energ, Oak Ridge, Tenn., USA, 1994.

Masiello, C. A., Chadwick, O. A., Southon, J., Torn, M. S., and Harden, J. W.: Weathering controls on mechanisms of carbon storage in grassland soils, Global Biogeochem. Cy., 18, GB4023, doi:10.1029/2004GB002219, 2004.

McMurtrie, R. E., Iversen, C. M., Dewar, R. C., Medlyn, B. E., Näsholm, T., Pepper, D. A., and Norby, R. J.: Plant root distributions and nitrogen uptake predicted by a hypothesis of optimal root foraging, Ecology and Evolution, 2, 1235–1250, doi:10.1002/ece3.266, 2012.

Niu, G.-Y. and Yang, Z.-L.: Effects of Frozen Soil on Snowmelt Runoff and Soil Water Storage at a Continental Scale, Journal of Hydrometeorology, 7, 937–952, 2006.

Nydal, R. and Lövseth, K.: Carbon-14 Measurements In Atmospheric CO_2 From Northern And Southern Hemisphere Sites, 1962–1993, NDP 057, Carbon Dioxide Information Analysis Center, 1996.

O'Brien, B. and Stout, J.: Movement and turnover of soil organic matter as indicated by carbon isotope measurements, Soil Biol. Biochem., 10, 309–317, 1978.

Oleson, K. W., Lawrence, D. M., Bonan, G. B., Flanner, M. G., Kluzek, E., Lawrence, P. J., Levis, S., Swenson, S. C., Dai, P. E. T. A., Decker, M., Dickinson, R., Feddema, J., Heald, C. L., Hoffman, F., Lamarque, J., Mahowald, N., Niu, G., Qian, T., Randerson, J., Running, S., Sakaguchi, K., Slater, A., Stöckli, R., Wang, A., Yang, Z. L., Zeng, X., and Zeng, X.: Technical Description of version 4.0 of the Community Land Model (CLM), NCAR TECHNICAL NOTE #NCAR/TN-478+STR, 2010.

Parton, W., Stewart, J., and Cole, C.: Dynamics of C, N, P And S in Grassland Soils – A Model, Biogeochemistry, 5, 109–131, 1988.

Parton, W., Mosier, A., Ojima, D., Valentine, D., Schimel, D., Weier, K., and Kulmala, A.: Generalized model for N_2 and N_2O production from nitrification and denitrification, Global Biogeochem. Cy., 10, 401–412, 1996.

Parton, W. J., Holland, E. A., Grosso, S. J. D., Hartman, M. D., Martin, R. E., Mosier, A. R., Ojima, D. S., and Schimel, D. S.: Generalized model for NO_x and N_2O emissions from soils, J. Geophys. Res., 106, 17403–17419, doi:10.1029/2001JD900101, 2001.

Ping, C.-L., Michaelson, G. J., Jorgenson, M. T., Kimble, J. M., Epstein, H., Romanovsky, V. E., and Walker, D. A.: High stocks of soil organic carbon in the North American Arctic region, Nat. Geosci., 1, 615–619, doi:10.1038/ngeo284, 2008.

Qian, H., Joseph, R., and Zeng, N.: Enhanced terrestrial carbon uptake in the Northern High Latitudes in the 21st century from the Coupled Carbon Cycle Climate Model Intercomparison Project model projections, Glob. Change Biol., 16, 641–656, doi:10.1111/j.1365-2486.2009.01989.x, 2010.

Qian, T., Dai, A., Trenberth, K. E., and Oleson, K. W.: Simulation of global land surface conditions from 1948 to 2004. Part I: Forcing data and evaluations, J. Hydrometeorol., 7, 953–975, 2006.

Rappoldt, C. and Crawford, J.: The distribution of anoxic volume in a fractal model of soil, Geoderma, 88, 329–347, 1999.

Richards, P. J. and Humphreys, G. S.: Burial and turbulent transport by bioturbation: a 27-year experiment in southeast Australia, Earth Surf. Proc. Land., 35, 856–862, doi:10.1002/esp.2007, 2010.

Riley, W. J., Gaudinski, J. B., Torn, M. S., Joslin, J. D., and Hanson, P. J.: Fine-root mortality rates in a temperate forest: estimates using radiocarbon data and numerical modeling, New Phytol., 184, 387–398, doi:10.1111/j.1469-8137.2009.02980.x, 2009.

Riley, W. J., Subin, Z. M., Lawrence, D. M., Swenson, S. C., Torn, M. S., Meng, L., Mahowald, N. M., and Hess, P.: Barriers to predicting changes in global terrestrial methane fluxes: analyses using CLM4Me, a methane biogeochemistry model integrated in CESM, Biogeosciences, 8, 1925–1953, doi:10.5194/bg-8-1925-2011, 2011.

Schaefer, K., Zhang, T., Bruhwiler, L., and Barrett, A. P.: Amount and timing of permafrost carbon release in response to climate warming, Tellus B, 63, 165–180, doi:10.1111/j.1600-0889.2011.00527.x, 2011.

Sierra, C. A., Harmon, M. E., Thomann, E., Perakis, S. S., and Loescher, H. W.: Amplification and dampening of soil respiration by changes in temperature variability, Biogeosciences, 8, 951–961, doi:10.5194/bg-8-951-2011, 2011.

Stuiver, M. and Polach, H.: Reporting of 14C data, Radiocarbon, 19, 355–363, 1977.

Swenson, S. C. and Lawrence, D. M.: A new fractional snow-covered area parameterization for the Community Land Model and its effect on the surface energy balance, J. Geophys. Res., 117, D21107, doi:10.1029/2012JD018178, 2012.

Swenson, S. C., Lawrence, D. M., and Lee, H.: Improved simulation of the terrestrial hydrological cycle in permafrost regions by the Community Land Model, J. Adv. Model. Earth Syst., 4, M08002, doi:10.1029/2012MS000165, 2012.

Tang, J. Y., Riley, W. J., Koven, C. D., and Subin, Z. M.: CLM4-BeTR, a generic biogeochemical transport and reaction module for CLM4: model development, evaluation, and application, Geosci. Model Dev., 6, 127–140, doi:10.5194/gmd-6-127-2013, 2013.

Tarnocai, C., Swanson, D., Kimble, J., and Broll, G.: Northern Circumpolar Soil Carbon Database, Digital database, Research Branch, Agriculture and Agri-Food Canada, Ottawa, Canada, 2007.

Tarnocai, C., Canadell, J. G., Schuur, E. A. G., Kuhry, P., Mazhitova, G., and Zimov, S.: Soil Organic Carbon Pools in the Northern Circumpolar Permafrost Region, Global Biogeochem. Cy., 23, GB2023, doi:10.1029/2008GB003327, 2009.

Thomas, R. Q., Bonan, G. B., and Goodale, C. L.: Insights into mechanisms governing forest carbon response to nitrogen deposition: a model-data comparison using observed responses to nitrogen addition, Biogeosciences Discuss., 10, 1635–1683, doi:10.5194/bgd-10-1635-2013, 2013.

Thornton, P. and Rosenbloom, N.: Ecosystem model spin-up: Estimating steady state conditions in a coupled terrestrial carbon and nitrogen cycle model, Ecol. Model., 189, 25–48, doi:10.1016/j.ecolmodel.2005.04.008, 2005.

Thornton, P. E., Lamarque, J.-F., Rosenbloom, N. A., and Mahowald, N. M.: Influence of carbon-nitrogen cycle coupling on land model response to CO_2 fertilization and climate variability, Global Biogeochem. Cy., 21, doi:10.1029/2006GB002868, 2007.

Thornton, P. E., Doney, S. C., Lindsay, K., Moore, J. K., Mahowald, N., Randerson, J. T., Fung, I., Lamarque, J.-F., Feddema, J. J., and Lee, Y.-H.: Carbon-nitrogen interactions regulate climate-carbon cycle feedbacks: results from an atmosphere-

ocean general circulation model, Biogeosciences, 6, 2099–2120, doi:10.5194/bg-6-2099-2009, 2009.

Todd-Brown, K. E. O., Randerson, J. T., Post, W. M., Hoffman, F. M., Tarnocai, C., Schuur, E. A. G., and Allison, S. D.: Causes of variation in soil carbon simulations from CMIP5 Earth system models and comparison with observations, Biogeosciences, 10, 1717–1736, doi:10.5194/bg-10-1717-2013, 2013.

Torn, M. S., Lapenis, A. G., Timofeev, A., Fischer, M. L., Babikov, B. V., and Harden, J. W.: Organic carbon and carbon isotopes in modern and 100-year-old-soil archives of the Russian steppe, Glob. Change Biol., 8, 941–953, doi:10.1046/j.1365-2486.2002.00477.x, 2002.

Trumbore, S., Vogel, J., and Southon, J.: AMS C-14 Measurements Of Fractionated Soil Organic-Matter – An Approach To Deciphering The Soil Carbon-Cycle, Radiocarbon, 31, 644–654, 1989.

Trumbore, S., Davidson, E., Decamargo, P., Nepstad, D., and Martinelli, L.: Belowground Cycling Of Carbon In Forests And Pastures Of Eastern Amazonia, Global Biogeochem. Cy., 9, 515–528, 1995.

Turnbull, J. C., Lehman, S. J., Miller, J. B., Sparks, R. J., Southon, J. R., and Tans, P. P.: A new high precision (CO_2)-^{14}C time series for North American continental air, J. Geophys. Res.-Atmos., 112, D11310, doi:10.1029/2006JD008184, 2007.

Wang, Y.-P. and Houlton, B. Z.: Nitrogen constraints on terrestrial carbon uptake: Implications for the global carbon-climate feedback, Geophys. Res. Lett., 36, L24403, doi:10.1029/2009GL041009, 2009.

Wang, Y. P., Law, R. M., and Pak, B.: A global model of carbon, nitrogen and phosphorus cycles for the terrestrial biosphere, Biogeosciences, 7, 2261–2282, doi:10.5194/bg-7-2261-2010, 2010.

Wania, R., Ross, I., and Prentice, I. C.: Integrating peatlands and permafrost into a dynamic global vegetation model: 2. Evaluation and sensitivity of vegetation and carbon cycle processes, Global Biogeochem. Cy., 23, GB3015, doi:10.1029/2008GB003413, 2009.

Xia, J. Y., Luo, Y. Q., Wang, Y.-P., Weng, E. S., and Hararuk, O.: A semi-analytical solution to accelerate spin-up of a coupled carbon and nitrogen land model to steady state, Geosci. Model Dev., 5, 1259-1271, doi:10.5194/gmd-5-1259-2012, 2012.

Yoo, K., Ji, J., Aufdenkampe, A., and Klaminder, J.: Rates of soil mixing and associated carbon fluxes in a forest versus tilled agricultural field: Implications for modeling the soil carbon cycle, J. Geophys. Res., 116, G01014, doi:10.1029/2010JG001304, 2011.

Zaehle, S., Friedlingstein, P., and Friend, A. D.: Terrestrial nitrogen feedbacks may accelerate future climate change, Geophys. Res. Lett., 37, L01401, doi:10.1029/2009GL041345, 2010.

Zeng, X.: Global vegetation root distribution for land modeling, J. Hydrometeorol., 2, 525–530, 2001.